

**ADDIS ABABA UNIVERSITY**  
**ADDIS ABABA INSTITUTE OF TECHNOLOGY**  
**SCHOOL OF CIVIL AND ENVIRONMENTAL ENGINEERING**



**EFFECTS OF LOSS OF BOND ON THE SHEAR BEHAVIOR  
OF SLENDER REINFORCED CONCRETE BEAMS**

---

**A Thesis in Structural Engineering**

By Akililu Abraham

September 2021

Addis Ababa, Ethiopia

A Thesis

Submitted to in Partial Fulfillment of the Requirements for the Degree of Master of Science.

The undersigned have examined the thesis entitled “**Effects of Loss of Bond on the Shear Behavior of Slender Reinforced Concrete Beams**” presented by **Akililu Abraham** a candidate for the degree of **Master of Science** and hereby certify that it is worthy of acceptance.

Dr. Esayas Gebreyouhannes	_____	_____
Advisor	Signature	Date
Dr.-Ing. Adil Zekaria	_____	_____
Internal Examiner	Signature	Date
Prof. Girma Zerayohannes	_____	_____
External Examiner	Signature	Date
Dr.-Ing. Mebruk Mohammed	_____	_____
Chair person	Signature	Date

## **DEDICATION**

This thesis is dedicated to

My sister Shega,

My father Abraham, and

My grandfather Botto.

## **UNDERTAKING**

I, the undersigned declare that “effects of loss of bond on the shear behavior of slender reinforced concrete beams” is the result of my own effort and has not been presented elsewhere for assessment, and that all sources used for the thesis have been duly acknowledged.

Akililu Abraham

## ABSTRACT

This study investigates the shear behavior of slender reinforced concrete beams, which were fabricated with loss of bond between main longitudinal reinforcement and surrounding concrete. To remove the bond effect, the reinforcements were inserted into a plastic pipe, and then they were properly anchored behind the supports to control excessive slip. Four simply supported beams were tested under monotonic loading: one with full bond and three with the varied bond length between concrete-rebar interfaces.

The test results show that the loss of bond has significant effects on crack patterns, mode of failure and ultimate load-carrying capacity. In a full span unbonded beam, only two flexural cracks were formed before failure and the mode of failure changed from shear to flexure. In partially unbonded beams, the formed failure inclined cracks are found to be steeper than the reference beam failure inclined cracks, and these cracks crossed the shear span of the beam at the end of unbonded length. Also, the failure inclined crack patterns and mode of failure are found to be similar, in partially unbonded beams. Besides, the test results show that the loss of bond has significant effects on the load-carrying capacity of beams. The ultimate load-carrying capacity has been varied depending on the percentage of unbonded length in the shear span of the beam. In the fully unbonded beam, the ultimate load-carrying capacity had increased whereas it has decreased in the case of partially unbonded beams when compared to the reference beam. However, increasing the percentage of debonding length enhanced the carrying capacity of the beams. Finally, the flexural stiffness of beams decreases as the percentage of loss of bond increases.

**Keywords:** Shear behavior, slender beam, and loss of bond.

## **ACKNOWLEDGMENTS**

First of all, I would like to thank my Almighty God for giving me strength and patience to accomplish my work.

I would like to thank my advisor, Dr. Esayas Gebreyouhannes for his supports.

I would also like to thank my family for their moral supports.

I am also thankful to my uncle Yonas Amanuel for his continuous supports to complete this study.

Finally, my deepest thanks go to my friends for their help during this work.

## TABLE OF CONTENTS

<b>DEDICATION .....</b>	<b>I</b>
<b>UNDERTAKING .....</b>	<b>II</b>
<b>ABSTRACT.....</b>	<b>III</b>
<b>ACKNOWLEDGMENTS .....</b>	<b>IV</b>
<b>TABLE OF CONTENTS .....</b>	<b>V</b>
<b>LIST OF TABLES .....</b>	<b>VIII</b>
<b>LIST OF FIGURES .....</b>	<b>IX</b>
<b>NOTATIONS .....</b>	<b>XI</b>
<b>CHAPTER 1 INTRODUCTION.....</b>	<b>1</b>
1.1 Background of the Study.....	1
1.2 Statement of the Problem.....	2
1.3 General Objective.....	3
1.3.1 Specific Objective.....	3
1.4 Significance of the Study .....	3
1.5 Scope of the Study .....	3
1.6 Organization of the Thesis .....	4
<b>CHAPTER 2 LITERATURE REVIEW.....</b>	<b>5</b>
2.1 General overviews.....	5
2.2 Shear Force Transfer Mechanism .....	5
2.2.1 Effects of Shear Span to Depth Ratio on Shear Behavior .....	8
2.2.2 Shear Failure Modes .....	9
2.3 Bond Behavior of Reinforced Concrete .....	13
2.3.1 Bond Force Transfer Mechanism .....	14
2.3.2 Factors Affecting Bond of Reinforced Concrete .....	16
2.3.3 Summary of the Factors that Affect Bond .....	22
2.4 Effects of Loss of Bond in Reinforced Concrete .....	22
<b>CHAPTER 3 EXPERIMENTAL PROGRAM .....</b>	<b>25</b>

3.1	General .....	25
3.2	Details of Specimens .....	25
3.3	Property of Materials.....	27
3.3.1	Concrete .....	27
3.3.2	Reinforcement.....	30
3.4	Fabrication of Specimens .....	31
3.4.1	Preparation of Reinforcements Cages.....	31
3.4.2	Preparation of Formwork.....	32
3.4.3	Casting of Concrete .....	33
3.5	Test Setup .....	34
3.6	Instrumentation and Data Acquisition.....	35
<b>CHAPTER 4</b>	<b>FINITE ELENRMT ANALYSIS USING VecTor2 .....</b>	<b>36</b>
4.1	About the Software .....	36
4.2	Material Models .....	36
4.2.1	Concrete Models .....	37
4.2.2	Reinforcement Models.....	38
4.2.3	Bond Models.....	38
4.3	Analysis Models.....	39
4.4	Material Properties.....	39
4.5	Specimens .....	40
4.6	Analysis of Finite Element Model .....	40
<b>CHAPTER 5</b>	<b>RESULTS AND DISCUSSION.....</b>	<b>41</b>
5.1	General .....	41
5.2	Experimental Results .....	41
5.2.1	Full Span Bonded Beam (BUL0).....	41
5.2.2	One-Third of the Span Unbonded Beam (BUL1).....	43
5.2.3	Two-Third of the Span Unbonded Beam (BUL2) .....	44
5.2.4	Full Span Unbonded Beam (BUL3) .....	45
5.3	Discussion of Results .....	47
5.4	Finite Element Results .....	49

<b>CHAPTER 6</b>	<b>CONCLUSION AND RECOMMENDATION.....</b>	<b>52</b>
6.1	Conclusion.....	52
6.2	Recommendation.....	53
<b>APPENDIX A:</b>	<b>CONCRETING MATERIALS TESTS .....</b>	<b>58</b>
<b>APPENDIX B:</b>	<b>MECHANICAL PROPERTY OF MATERIALS.....</b>	<b>61</b>

## LIST OF TABLES

Table 3-1: Quantity of materials for mix proportion per cubic meter of concrete .....	28
Table 3-2: Summary of the concrete strength.....	30
Table 3-3: Mechanical properties of reinforcements .....	31
Table 4-1: Summary of the used modeling option for concrete .....	37
Table 4-2: Used analysis model.....	39
Table 5-1: Summary of test results .....	47
Table 5-2: Summary of peak loads and their variation from the reference beam .....	49
Table 5-3: Peak load comparison of experimental and analytical results.....	51

## LIST OF FIGURES

Figure 2-1: Average shear stress between cracks [10] .....	6
Figure 2-2: Effect of shear span to depth ratio on shear behavior [10] .....	8
Figure 2-3: Diagonal tension failure mode [18] .....	10
Figure 2-4: Shear –compression failure mode [10] .....	11
Figure 2-5: Shear –tension failure mode [10] .....	12
Figure 2-6: Splitting of concrete behind the support [18] .....	12
Figure 2-7: arch action in beams [10] .....	12
Figure 2-8: Bond force transfer mechanism [10].....	16
Figure 2-9: Typical splitting surfaces [10] .....	16
Figure 2-10: Corrosion effect on bond strength [24] .....	17
Figure 3-1: Full span bonded beam .....	26
Figure 3-2: One-third of the span unbonded beam.....	26
Figure 3-3: Two-third of the span unbonded beam .....	26
Figure 3-4: Full span unbonded beam .....	26
Figure 3-5: typical cross-section of a beam.....	27
Figure 3-6: Compressive strength test .....	29
Figure 3-7: Splitting test of cylindrical specimen.....	29
Figure 3-8: Tensile strength test of reinforcement.....	30
Figure 3-9: Reinforcement cage of full span bonded beam.....	31
Figure 3-10: Reinforcement cage of one-third of the span unbonded beam .....	32
Figure 3-11: Reinforcement cage of two-third of the span unbonded beam .....	32
Figure 3-12: Reinforcement cage of full span unbonded beam.....	32
Figure 3-13: Reinforcement cages inside the formwork .....	33
Figure 3-14: Concrete placing process .....	<b>Error! Bookmark not defined.</b>
Figure 3-15: Test set up .....	34
Figure 4-1; Eligehausen bond stress-slip response .....	38
Figure 4-2: Typical model of finite element.....	40
Figure 5-1: Failure mode of BUL0 .....	42
Figure 5-2: Load versus deflection curve of BUL0 .....	42
Figure 5-3: Failure mode of BUL1 .....	43
Figure 5-4: Load versus deflection curve of BUL1 .....	44
Figure 5-5: Failure mode of BUL2 .....	45

Figure 5-6: Load versus deflection curve of BUL2 .....	45
Figure 5-7: Failure mode of BUL3 .....	46
Figure 5-8: Load versus deflection curve of BUL3 .....	46
Figure 5-9: Load versus deflection curve of all beams.....	49
Figure 5-10: Experimental and analytical load versus deflection curves of BUL0.....	50
Figure 5-11: Experimental and analytical load versus deflection curves of BUL1 .....	50
Figure 5-12: Experimental and analytical load versus deflection curves of BUL2 .....	51
Figure 5-13: Experimental and analytical load versus deflection curves of BUL3 .....	51

## NOTATIONS

ACI: American concrete institute

ASTM: American society for testing materials

EBCS: Ethiopian building code of standard

BUL0: Full span bonded beam

BUL1: One-third of the span unbonded beam

BUL2: Two-third of the span unbonded beam

BUL3: Full span unbonded beam

LVDT: Linear variable differential transducer

RC: Reinforced concrete

## CHAPTER 1

### INTRODUCTION

#### 1.1 Background of the Study

Structural concrete functions effectively as a composite material because the reinforcement is bonded to the surrounding concrete. Bond ensures that there is little or no slip of the rebar relative to the concrete and hence allows local forces to be transferred across the concrete-rebar interface [1, 2]. Therefore, for the satisfactory performance of reinforced concrete structures, the adequate bond strength between reinforcement and concrete is important [3].

The bond strength of reinforced concrete structures can deteriorate during service as it is subjected to various types of loads. The load types that can deteriorate bond strength are illustrated as follows:

The effects of cyclic load on the operational properties of reinforced concrete structures are more intense, complex, and dangerous for safety than that of static loads. Moreover, increasing the number of load cycles on the same structure accumulates damage on component materials and the bond between them. Finally, after some number of cycles, the bond strength between the reinforcement and concrete will deteriorate, and then the reinforcement starts to slip and deflection of structure increases [4, 5].

Corrosion of the reinforcement due to the presence of moisture is another factor that can affect bond strength. Because corroded reinforcement occupies a large volume than the original one, which induces pressure on surrounding concrete. Then it causes cracking of concrete if the volumetric expansion on concrete is greater than the tensile strength of concrete. Finally, it resulted in the loss of the bond [6]. Also, corrosion of the reinforcement has a significant effect on the cyclic performance of reinforced concrete beams due to bond degradation between concrete- rebar interfaces [7].

In general, due to corrosion of reinforcement and cyclic loads, the bond between concrete-rebar interfaces will be lost during service; however, reinforced concrete is modeled considering the full bond strength.

Loss of bond changes the load transfer mechanism from a combined beam and arch action to arch action. Accordingly, it changes the ultimate load-carrying capacity of beams that are designed to fail in shear [8]. In addition, it changes the ultimate load-carrying capacity for beams that are designed to fail in flexure [9].

Shear failure is one of the failure mechanisms that needs an extensive evaluation of its actual behavior because of its undesirable mode of failure. Slender beams, which are focused in this study, are weak in shear resistance than deep beams. This is because in the latter case, shear stress is transferred by diagonal compression of a concrete strut, but such stress transfer mechanism does not exist in the slender beams. Moreover, unlike deep beams, in slender beams bond force between reinforcement and concrete is essential for horizontal stress flow between cracks from tensile reinforcement to an uncracked zone of compression concrete. In other words, loss of bond in slender beam disrupts the transfer of shear force by beam action [10]. Thus, loss of bond in slender beams by any means will disrupt the horizontal stress flow, and then it results in a new stress flow if the load increases further.

Therefore, a deep investigation is needed for structures with loss of bond during service time, particularly for the shear behavior of slender beams to know actual performance and failure mechanism after the loss of bond strength.

In this study, both experimental test and finite element analysis were performed to investigate the shear behavior of slender reinforced concrete beams by varying the unbonded length of main longitudinal reinforcement. To create the loss of bond, the longitudinal tension reinforcements were inserted into a plastic pipe, and they were properly anchored behind the supports to control excessive slip.

## **1.2 Statement of the Problem**

The influence of loss of bond between reinforcement and surrounding concrete during service time of reinforced concrete structure is not yet comprehensively understood. In codes of practice, a perfect bond is considered to design. But such consideration may not be corrected during service time for the reason that bond strength variations will exist between design bond strength and residual bond strength after the loss of bond. Because in different researchers investigation, results show that the bond strength starts to decrease

with further increase of corrosion and cyclic loads. Thus, the shear behavior of reinforced concrete structures such as crack pattern, mode of failure, and ultimate load-carrying capacity will not know after the loss of bond.

### **1.3 General Objective**

The general objective of this research is to investigate the effects of loss of bond between main longitudinal reinforcement and surrounding concrete on the shear behavior of slender reinforced concrete beams to improve understanding of the shear behavior of reinforced concrete structures.

#### **1.3.1 Specific Objective**

To examine the shear behavior of reinforced concrete beams with varying percentages of unbonded length between reinforcement and concrete interfaces.

### **1.4 Significance of the Study**

This study aims to identify the gap between the behavior of structures that model considering a perfect bond strength and the actual behavior of structures after the damage of bond. Because the existing models do not incorporate the verification methods with residual bond strength after bond degradation. That means the effect of loss of bond is not addressed in current codes of practice. Therefore, this study will serve as a springboard for researchers to revise the existing bond strength verification methods, which should be taken into account for the future loss of the bond.

### **1.5 Scope of the Study**

To achieve the objective of this study, four simply supported slender reinforced concrete beams with a shear span to depth ratio of 3.12 were fabricated, and then tested with monotonically applied load. The effects of different grades of concrete and reinforcements were not considered. However, all beams were designed to fail in shear. Besides, the insertion of reinforcements into a plastic pipe is only the used method to create the loss of the bond.

## 1.6 Organization of the Thesis

This section presents the structure of the thesis. The thesis has been organized into five chapters.

Chapter one deals with the background of the study, statement of the problem, objectives, significance of the study, limitation of the study, and organization of the thesis.

Chapter two reviews the literature on the general shear behavior, shear load transfer mechanisms on reinforced concrete structures with the effect of slenderness ratio, and shear failure modes. In addition, it reviews bond behavior of reinforced concrete structures with bond force transfer mechanism and the factors that affect bond strength between reinforcement and surrounding concrete and finally the effects of loss of bond in reinforced concrete structures.

Chapter three presents the experimental program including a general overview, details of fabricated specimens, properties of used materials, fabrication methods of specimens, test setup, instrumentation, and data question.

Chapter four presents the materials models for finite element analysis, materials properties for finite element analysis and specimens for finite element analysis.

Chapter five presents the experimental results obtained from the monotonic loading test, discussion on the effect of loss of bond on shear behavior of tested beams and results of finite element analysis.

The last chapter, chapter five, presents conclusions and recommendations for the study.

## CHAPTER 2

### LITERATURE REVIEW

#### 2.1 General overviews

Bond deterioration between reinforcement and surrounding concrete affects the shear behavior of structures [8]. This complicates the exact prediction of a single rationally accepted equation [11, 12] in building codes of practice [13, 14, 15]. This is because bond strength continuously reduces during service time even if a basic assumption made for concrete design is not tolerated the relative movement between reinforcement and concrete interfaces. This means reinforcement and concrete must be combined by constant bond strength throughout the design period.

This chapter overviews the shear and bond, and shear transfer mechanisms including the effects of shear span to depth ratio on transfer mechanisms and modes of failure in shear. It also presents bond behaviors with factors affecting the bond strength of reinforced concrete members, bond force transfer mechanism, and effects of loss of bond strength on reinforced concrete members.

#### 2.2 Shear Force Transfer Mechanism

Based on the mechanism, in reinforced concrete beams, the shear force is transferred in both beam action and arch action. The shear span to depth ratio, which will be discussed in section 2.2.1, determines the extent of both beam and arch actions. The theoretical methods for shear transfer mechanisms can be expressed as follows:

Consider the free body diagram shown in figure 2.1b, which is the portion of a reinforced concrete beam between two cracks that is also the shaded area in figure 2.1a.

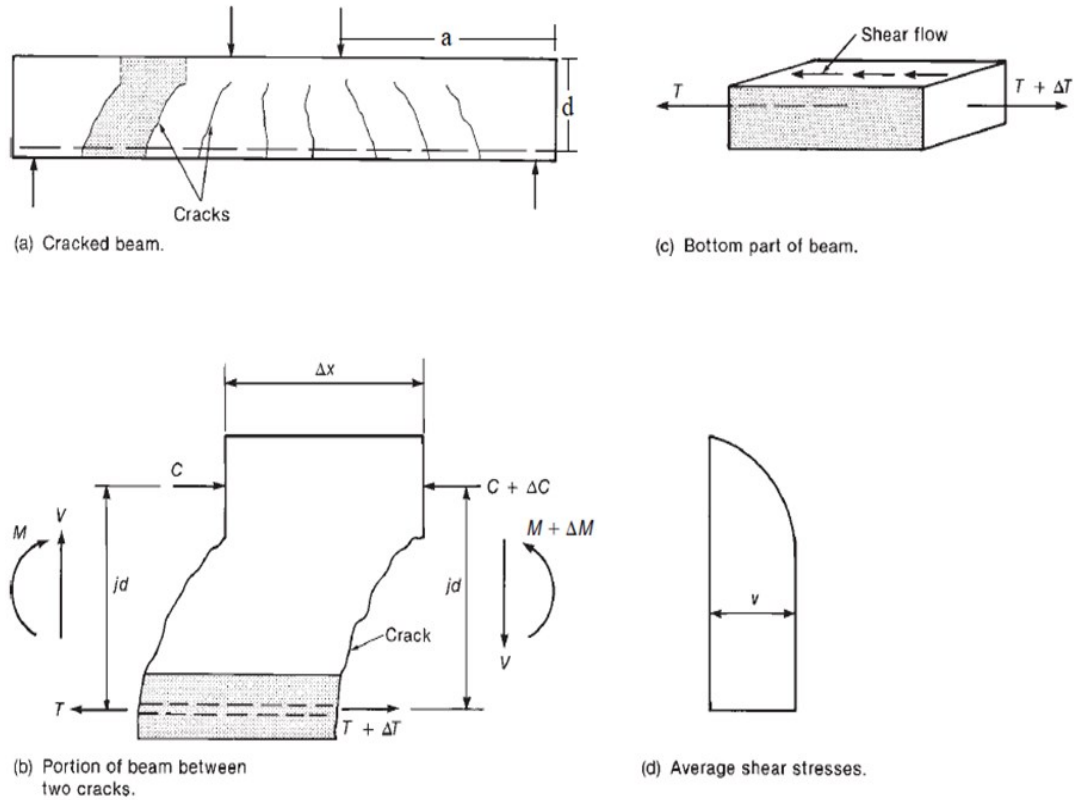


**Figure 2-1: Average shear stress between cracks [10]**

After the development of cracks, the equilibrium of the beam sections at both left and right cracks can be expressed as follows:

$$T = \frac{M}{jd} \quad \text{and} \quad T + \Delta T = \frac{M + \Delta M}{jd} \quad \text{respectively}$$

So that change of force in longitudinal tensile reinforcement is:

$$\Delta T = \frac{\Delta M}{jd} \tag{2.1}$$

Where  $jd$  is the flexural lever arm of the beam

Moment equilibrium for a portion of the element between two cracks can be also expressed as:

$$\Delta M = V\Delta X \tag{2.2}$$

Then, after substitution of equation 2.2 into equation 2.1

$$\Delta T = \frac{V\Delta X}{jd} \tag{2.3}$$

Also, consider the portion of the bottom part of the beam shown in figure 2-1c which is isolated from the shaded portion shown in figure 2-1b. In this isolated portion, the force ( $\Delta T$ ) transferred by horizontal shear stresses flows on the top surface of the isolated element. But, the average horizontal shear stresses value on the top surface of the bottom part of the beam is:

$$v = \frac{\Delta T}{b_w \Delta x} \quad (2.4)$$

Then, the shear stress flow is

$$v = \frac{\Delta T}{\Delta x} \quad (2.5)$$

Where  $jd) \cong 0.9d$  and  $b_w$  is the thickness of the beam.

The relation that exists between the shear force ( $V$ ) and the tensile force in the reinforcement ( $T$ ) in equations 2.3 can be rewritten as:

$$V = \frac{d}{dx} (Tjd) \quad (2.6)$$

That can be expanded as follows:

$$V = \frac{d}{dx} (T)jd + \frac{d}{dx} (jd)T \quad (2.7)$$

From equation 2.7 two cases can be identified.

In the first case if, the lever arm ( $jd$ ) is constant as normal elastic beam theory then

$$\frac{d}{dx} (jd)T = 0 \text{ and then } V = \frac{d}{dx} (T)jd$$

Where  $V$  is the shear force and  $d(T)/dx$  is the shear stresses flow across any horizontal plane between the reinforcement and uncracked concrete in the compression zone as shown in figure 2-1c. This form of shear flow must exist for beam action to exist in beams.

In the second case if  $d(T)/dx$  equals zero, or between cracks the tension force ( $T$ ) in the reinforcement constant, then the shear force is transferred in the arch action mechanism as shown in the following equations:

$$\frac{d}{dx} (T)jd = 0 \text{ and then } V = \frac{d}{dx} (jd)T$$

This case occurs when shear flow across the horizontal plane cannot be transmitted due to loss of bond or disrupted by an inclined crack, which extends from the load point to the reaction point. In this case, the shear force transfers to the supports by arch action, which enhances the shear load-carrying capacity [10].

### 2.2.1 Effects of Shear Span to Depth Ratio on Shear Behavior

The shear behavior of reinforced concrete beams highly varied with shear span to depth ratio as shown in figure 2.2. Shear spans with shear span to depth ratio between 2 and 2.5 have a major variation in shear behavior. Moreover, it highly influences ultimate shear carrying capacity for shear span to depth ratio less than 2; however, it has little effect on inclined cracking. In the case of longer shear spans, it has a little effect on both the inclined cracking shear and failure shear capacity. If the shear span to depth ratio is greater than 6.5, failure occurs by flexure [10].

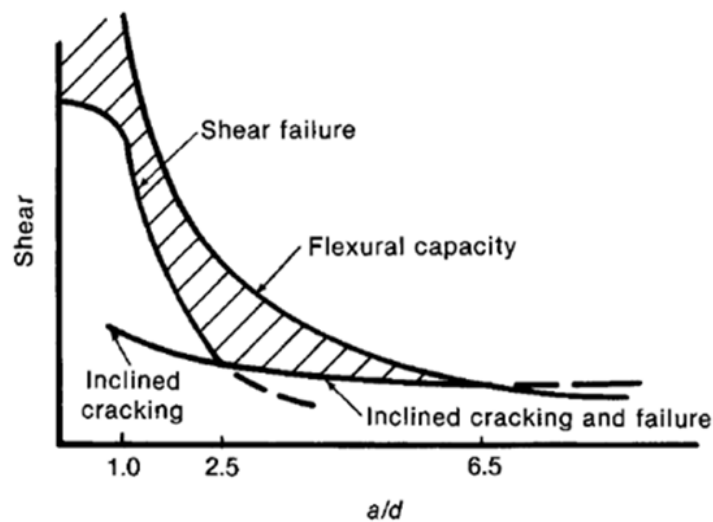


Figure 2-2: Effect of shear span to depth ratio on shear behavior [10]

According to Wight and MacGregor [10], the shear span to depth ratio of the beam is the dominant load transfer mechanism that was discussed in section 2.2. Beam action governs load transfer mechanism in the span to depth ( $a/d$ ) ratio greater than 2.5, and these beams are called slender beams. Whereas arch action governs load transfer mechanism using compressive struts of the concrete when the ratio is less than 2.5, and these beams are called deep beams. Sinik and Arslan [16] conducted an experimental investigation on the effect of shear span to depth ratio ( $a/d$ ) on the shear strength of reinforced concrete beams with shear reinforcement. Three beams with shear span to depth ratios ( $a/d$ ) of 2.5, 3.5, and 4.5 were tested applying concentrated load at mid-span. It was observed that the shear

strength of the tested beams decreased as the shear span to depth ratio ( $a/d$ ) increased. The authors concluded that increasing the shear span to depth ratio ( $a/d$ ) had a considerable effect on the mode of failure, which also change the failure mode from shear failure to flexural failure [16].

### **2.2.2 Shear Failure Modes**

Failure in shear occurs when the shear resistance of the beam is less incapable than the flexural strength of the beam and applied shear force exceeds the shear capacity of the beam at the shear critical section. Shear failure modes are an undesirable mode of failure, therefore most of the time shear reinforcement is used to enhance shear carrying capacity when shear resistance of concrete is lower than applied shear force. Shear failure modes were classified based on the distance between the loading point and reaction point concerning the effective depth of beams, which is also designated as the shear span to depth ratio of the beams. Diagonal tension failure occurs when shear span to depth ratio is more than 3 or 4 whereas shear-compression failure occurs when shear span to depth ratio between 1 and 2.5, and the anchorage failure mode is common if shear span to depth ratio between 0 and 1. In the following subsections, some of the shear failure modes are presented in-depth.

#### **2.2.2.1 Diagonal Tension Failure**

Diagonal crack, which occurs suddenly without giving warning, once formed propagates either at a high rate or low rate with increasing load, traversing a beam from the main reinforcement to compression face by splitting the beam into two parts and failing it. This type of crack occurs in beams when shear span to depth ratio eight and more [17]. Diagonal inclined crack in beam starts from the end of the last vertical crack and turns gradually into a diagonal direction which then cracks more inclined under the applied load as shown in figure 2.3. This crack does not immediately lead to failure, even though in some of the slender beams, it causes a failure. However, such crack is to be either the cause for failure or a new and flatter inclined crack formed which suddenly causes a failure. This crack encounters an increasing resistance as it propagates upwards into the compression zone of the beam, and it gets more flat at the same time and finally stopped at the point where it is marked at point “1”. Due to further loading, diagonal tension crack from point “1” gradually extends towards the load point at a very flat slope up to the point marked “2”. The extent of this crack behind the marked point “2” results in sudden failure. However,

before reaching the critical failure point “2”, additional inclined cracks will open back at bottom point “3” up to the reinforcement level and then followed by other cracks marked at point “4”. Cracks at points “3” & “4” are known as flexure shear cracks. In general, diagonal Tension failure mode occurs if the distance between load point and reaction point are far apart. It is common in beams with a shear span to depth ratio greater than 2. Sometimes it occurs at lower values [18].

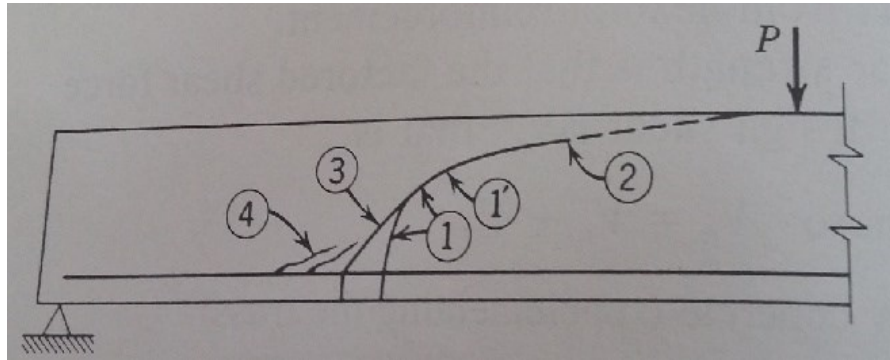


**Figure 2-3: Diagonal tension failure mode [18]**

#### **2.2.2.2 Shear Compression Failure**

In this case, the development and penetration of diagonal crack to the compression zone are stopped due to the presence of a nearby load as shown in figure 2.4. Because the vertical compressive stress under the point load reduces the possibility of further penetration of diagonal cracking, and the vertical compressive stresses over the reaction point, limit the splitting of bond along with the reinforcement. In I beams, shear compression failure mode occurs before a vertical flexural crack develops, in which a web-shear crack occurs across the neutral axis approximately a  $45^\circ$  due to a large shear in short shear spans. This web-shear crack crowds the shear resistance into a small depth of the beam, which is resulted in increasing stresses, then tends to be self-propagating until stopped by reaction or load point. Finally, a compression failure occurs next to the applied load. The location of concrete crushing takes place at the top of the diagonal crack of the beam around the area of the point load application as shown in figure 2.4. The shaded area near to the load carries most of the shear force; this is the reason to designate it as a shear-compression failure because, in this mode, failure is caused by the combination of shear and compression. Shear compression failure occurs in beams with a shear span to depth ratio less than four for normal strength concrete, but a little less for both lightweight and

high strength concrete [18]. Finally, failure occurs by crushing the compression zone, which occurs over the top of the diagonal crack [10].

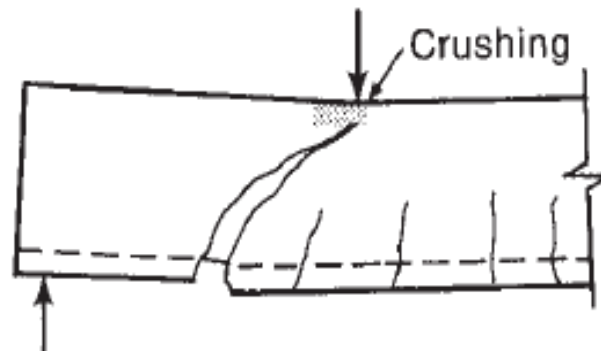


**Figure 2-4: Shear –compression failure mode [10]**

### ***2.2.2.3 Shear-Tension Failure***

Shear-tension failure occurs by splitting out of the reinforcement before compression failure if the longitudinal reinforcement beyond diagonal crack is not adequately anchored. Beams in this case act somewhat as a tied arch with a thrust line from point load, which needs full anchorage of reinforcement beyond the inclined crack. Therefore, shear reinforcements are required on most beams to eliminate splitting cracks [18]. Beams with the shear span to depth ratio between 1 and 2.5, initially develop inclined cracks, after redistribution of internal force to maintain equilibrium, and then carry the additional load by arch action. This type of failure mode is finally caused by a splitting of concrete cover along with reinforcement, bond failure and dowel failure along with the longitudinal reinforcement as shown in figure 2.5. Shear-tension failure can be common in the shear span to depth ratio between 1 & 2.5 [10]. Generally, shear tension failure occurs in beams if the flexural reinforcement at the anchorage zone begins to slip before shear compression failure occurs due to splitting crack of concrete cover. This will lose bond strength between concrete-rebar interfaces.

### ***2.2.2.4 Anchorage Failure***

This mode of failure common in a shear span to depth ratio is less than one. Shear force in beams with shear span to depth ratio less than one is carried by inclined thrust between reaction and load points, which eliminates diagonal tension. Finally, behind the support, the beam fails as splitting failure like the vertical splitting of compression test cylinder or it may fail in crushing of concrete at the reaction as shown in figure 2.6 [18]. In very short span beams (shear span to depth ratio between 0 and 1), loading develops inclined cracks

which join the load point and the support point. Due to further loading, these cracks in effect destroy the horizontal shear flow from the main reinforcement to the compression zone. Then, the longitudinal tensile reinforcement serves as the bottom chord of a tied arch so the tensile force in this chord is uniform between supports as shown in figure 2.7. Finally, the stress transfer mechanism changes from beam action to arch action [10].

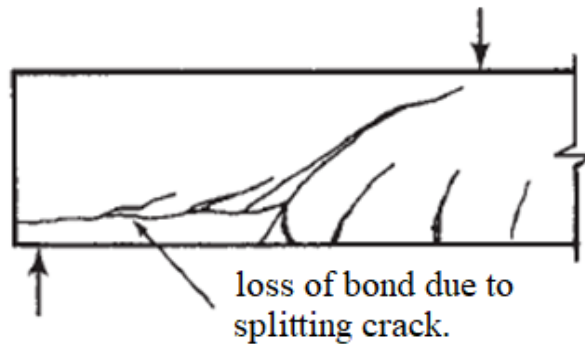


Figure 2-5: Shear –tension failure mode [10]

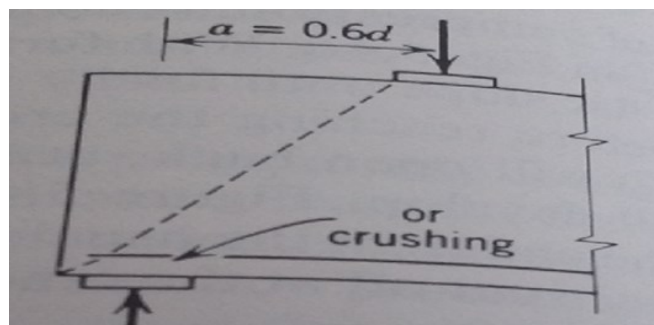


Figure 2-6: Splitting of concrete behind the support [18]

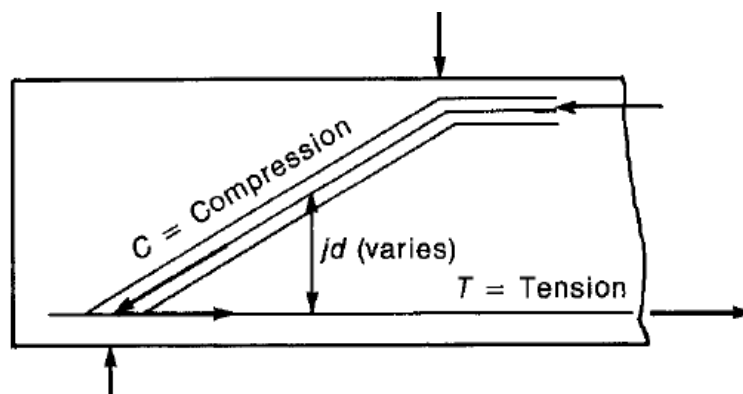


Figure 2-7: Arch action in beams [10]

### 2.3 Bond Behavior of Reinforced Concrete

Structures of reinforced concrete function effectively as a composite material because reinforcement and concrete are effectively bonded. The bond between reinforcement and concrete is used to ensure that there is no slip of the reinforcement relative to the surrounding concrete. Also, the bond allows the local stress transfer across the concrete-rebar interface. Without adequate bond strength, reinforcements in concrete are useless because the reinforcement does not contribute to beam capacity and the beam behaves like a plain concrete beam, and it fails immediately when the tensile strength of concrete is reached. Reinforcement transfer stresses across the interface or contributes to the structural performance if the reinforcement surrounded by concrete is properly anchored. Both local bond and end anchorage of the reinforcement plays a vital role in the strength of concrete structures. In general, the end anchorage is achieved in reinforced concrete beams due to the good bond conditions at the end of the beam, which closes to the supports and overhangs of the part behind the support [1].

The reinforced concrete that serves like another structural material is derived from the composite action effect of concrete that is weak in tension, but strong in compression and relatively durable, and reinforcements, which is strong and ductile in tension. To maintain composite action, transfer of load is required between reinforcement and surrounding concrete. This load transfer is known as the bond, and it is idealized as a continuous stress field that develops between concrete-rebar interfaces. Movement between the reinforcement and surrounding concrete is relatively little or no slip if the reinforced concrete member is subjected to a load that is less than the bond strength capacity. However, a significant movement between the reinforcement and surrounding concrete occurs that results in localized damage if the reinforced concrete member is subjected to a load that is greater than the bond strength capacity [2].

The external force is not applied directly to embedded reinforcement. Thus, reinforcements can receive their share of the load, which is transferred only from the surrounding concrete. Bond, which is used to transfer load between the reinforcement and surrounded concrete at the concrete-rebar interface, is important to modify the reinforcement stresses. An efficiently developed bond stress enables the reinforcement and concrete to form a composite structure. If the reinforcement stresses change between any two sections, bond stress will exist. Bond stresses develop in reinforced concrete members

in two distinct situations. The situations are the anchorage of reinforcements at the end and the change of reinforcement force due to change in bending moment along the structural member [19].

ACI Committee 408 [3] reported that satisfactory performance of reinforced concrete structures relies on adequate bond strength between reinforcement and concrete. Efficient and reliable stress transfer between reinforcement and concrete is required for the optimal design of reinforced concrete structures. In the report, bond strength depends on not only the materials but also the geometry of the reinforcement and structure itself. The transfer of bond stress from the reinforcement to surrounding concrete occurs in the deformed reinforcement [3]. According to the ACI committee 408 [3], the qualitative bond resistance depends on:

- Mechanical properties of concrete; which includes tensile and bearing strength properties,
- The volume of concrete that surrounds the reinforcement. This includes both concrete cover and spacing between adjacent reinforcements,
- Presence of transverse reinforcement as confinement, which is used to delay and control the early loading crack propagation,
- Surface conditions of reinforcements; and
- The geometry of reinforcements such as the height of ribs, spacing between ribs, the width of ribs, and the face angle of ribs.

### **2.3.1 Bond Force Transfer Mechanism**

The bond strength between the reinforcement and surrounding concrete is formed in three distinct components: mechanical friction from the roughness of interface, chemical adhesion between concrete-rebar interface, and bearing from deformed ribs against the concrete and surface irregularities on reinforcement. In the case of smooth reinforcements, friction and adhesion components contribute significantly to the bond strength. Contact pressure improves friction at the surface of the interface, and it increases with time due to the shrinkage of concrete. Furthermore, in the smooth reinforcement, roughness on the reinforcement surface and local irregularities in both size and shape influence bond

strength. In the case of deformed reinforcements, the presence of a pattern of deformations, which is rolled on the surface of the reinforcement, is the effective method of achieving a better bond. According to Warner et al. [1], the radial force component of the bearing force of deformed reinforcement contributes an important role for any bond failure, as it causes the longitudinal splitting of concrete if the tensile strength of the concrete cover and/ or tensile strength between adjacent reinforcements is less than the tensile strength of the radial component [1].

Bond force is developed by adhesion between concrete-rebar interface and friction in small amounts if the reinforcement embedded in concrete is smooth. Adhesion and friction effects quickly loss if tension load applies to the reinforcement. Because during loading the diameter of the reinforcement starts to decrease due to the Poisson effect. Friction and adhesion component of bond transfer mechanisms quickly loss at early stage loading of the deformed reinforcement even if the friction and adhesion action present, then the bond is resisted by bearing of the ribs of the reinforcement as shown in figure 2.8a. At the same time, equal but opposite in direction, bearing force acts on the surrounding concrete from deformed ribs as shown in figure 2.8b. The force on the concrete has two components: radial and longitudinal components as shown in figure 2.8 c and d. The former component causes circumferential tensile force in the concrete that surrounds the reinforcement. If this radial stress in the concrete exceeds the tensile strength of concrete, splitting of concrete starts at the interface parallel to the reinforcement. Then these cracks propagate outwards to the surface. As shown in figure 2.9, the splitting crack that developed in the beam follows the longitudinal reinforcement along the bottom face or side faces of the beam. Once the splitting cracks form, the bond force transfer mechanism drops immediately if reinforcement is not provided to control the opening of these cracks [10].

According to Wight and MacGregor [10], splitting failure load depends on;

- The smaller distance either from the distance between the reinforcement and the extreme surface of the concrete (thickness of concrete cover) or the distance between adjacent reinforcements,
- Tensile strength of concrete, and
- The average value of bond stress that less than the wedging forces. But splitting failure will occur if the average bond stress is greater than the wedging forces.

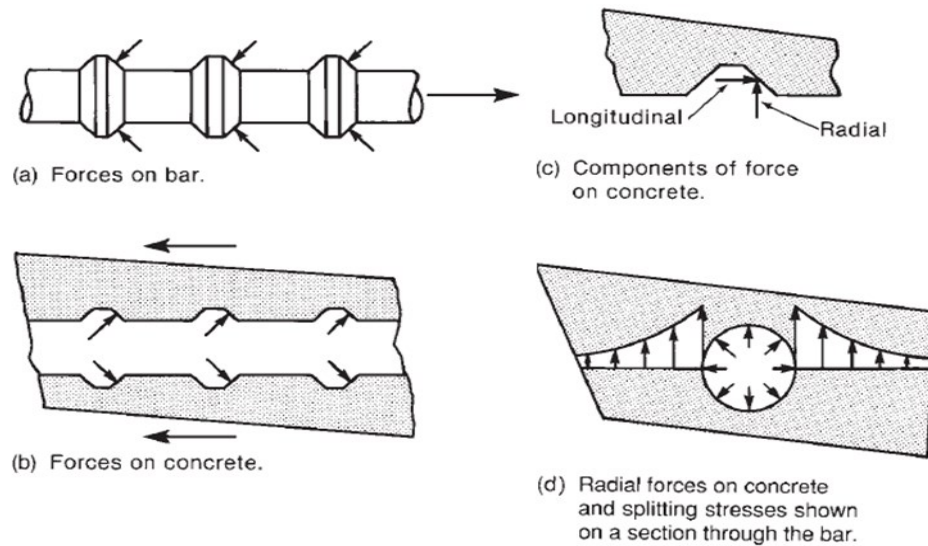


Figure 2-8: Bond force transfer mechanism [10]

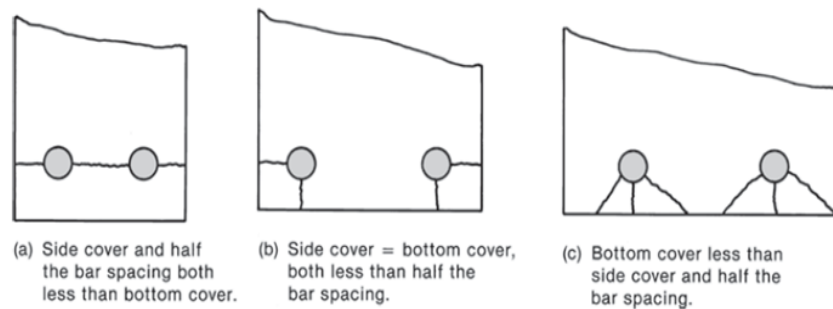


Figure 2-9: Typical splitting surfaces [10]

### 2.3.2 Factors Affecting Bond of Reinforced Concrete

The Bond-behavior of reinforcements embedded in concrete is affected by many factors. Environmental factors and improper detailing for the bond that deteriorate the bond strength are discussed in the following sections.

#### 2.3.2.1 Corrosion of Reinforcement

Corrosion of the reinforcement is one of the key factors that deteriorate the bond strength in concrete structures. Because, corroded reinforcement occupies a large volume than the original reinforcement, which induces volumetric expansion pressure on concrete that then causes tensile stresses in concrete. When these tensile stresses exceed the tensile strength of the concrete, cracking occurs on concrete. Therefore, loss of bond happens between concrete-rebar interfaces and then load-carrying capacity reduces. In addition, strength and the serviceability of reinforced concrete are greatly affected by corrosion of reinforcement, which leads a structure to accelerated aging [6]. Similarly, corrosion leads to cracking of

concrete cover, reduction of the cross-sectional area of reinforcement, and reduction of the bond between concrete-rebar interfaces [20].

An experimental investigation was carried out on the effects of corrosion of the reinforcement on the bond strength of reinforced concrete structures. The result indicates that the bond strength increases at the beginning with an increase in the percent of corrosion until the development of cracks in concrete and then it starts to decrease with a further increase of the percent of corrosion [21, 22]. The effect of the variation in the degree of corrosion on bond strength between reinforcement and concrete is shown in figure 2.10 [23].

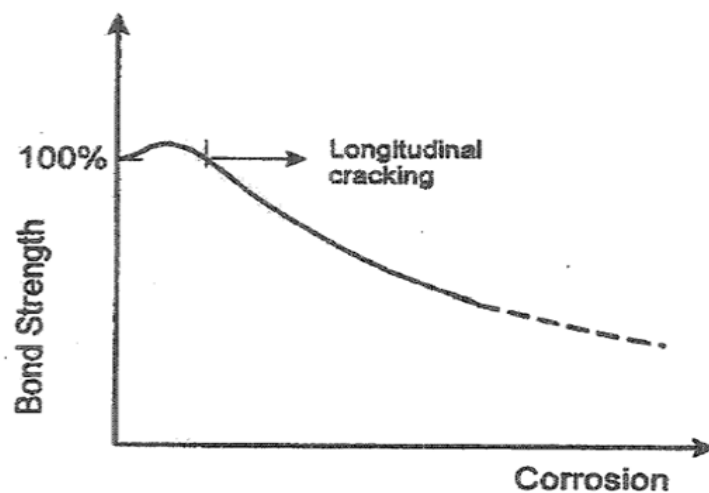


**Figure 2-10: Corrosion effect on bond strength [24]**

Amleh [24] conducted an experimental investigation on the effect of corrosion of reinforcements on the bond behavior between concrete-rebar interfaces. The type of tested specimens were standard tension specimens with a single reinforcement at its center. The reinforcement in the tension specimen was corroded using an accelerated corrosion method. Different levels of corrosion of the reinforcements were formed ranging from zero corrosion level to complete corrosion level at the concrete-rebar interface. Then tension specimens were subjected to axial tensions force after corrosion of reinforcement. The test result showed that the bond strength between concrete-rebar interface decreases as corrosion level increases. In the case of severe corrosion, the bond strength decreases rapidly. The author concluded that the bond strength at the deformed concrete-rebar interface decreases because of the widely opened crack at the longitudinal splitting of concrete [24].

The structural effects of reinforcement corrosion in reinforced concrete structures were studied to investigate the natural corrosion effect on service giving structures instead of artificially induced corrosion. The type of specimen was beam, which was taken from an old bridge's beams that also exist in an exposed environment. Specimens were categorized based on the extent of induced damage. Those are undamaged, medium damaged and highly damaged specimens. All specimens were indirectly supported by suspension hanger and then subjected to a four-point flexural test. In all specimens, similar behavior in the development of cracks and mode of failure were observed, which is splitting-induced pullout the failure mode. It was observed that the load-carrying capacity of the specimens with splitting cracks and spalling of concrete cover is lower than uncracked specimens are. It was also observed that the average calculated bond strength of the specimens with splitting cracks and spalling of concrete was reduced than uncracked specimens [25]. In general, the corrosion product of reinforcement exerts pressure within the concrete if that pressure exceeds the plastic deformation limit of the concrete. Then concrete cracks if the tensile strength of concrete is less the exerted pressure. Finally, cracked concrete resulted in a weakening bond strength [26].

### ***2.3.2.2 Cyclic Loading***

Ye et al. [27] conducted an experimental investigation on the effect of fatigue loading on the bond behavior between reinforcement and concrete. The type of test was pulled out with eccentric reinforcement that means 14mm diameter of the reinforcement was placed at the corner of 150 mm cube specimen size. And 6mm diameter plain reinforcement was also placed at the center of all specimens to confine the specimen. Then, fatigue loadings were applied to tested specimens with several cycles and amplitudes. The test result showed that all specimens were failed by splitting failure mode. It was observed that initially the fatigue load cycles enhance the bond strength until the critical bond strength; however, further increasing of fatigue load cycles decreases the bond strength because damage accumulation exceeds a critical value. It was also observed that a slip between reinforcement and concrete increases due to increasing numbers of fatigue load cycles which destroyed adhesion force between concrete-rebar interface, and the bond strength reach a critical value at early loading if fewer numbers of cycles with the large range of amplitude applied. The authors concluded that cyclic loading deteriorates the bond between reinforcement and concrete, interrupts the force transfer mechanism, increases the number of cracks, increases crack width, and decrease load-carrying capacity [27].

Rehm and Eligehausen [28] carried out a pullout test to examine the bond behavior of deformed reinforcements under high cycle repeating load conditions. The varied parameters of the study were the diameter of the reinforcement, maximum load, the amplitude of load and quality of concrete. Specimens were tested, and then they were failed by pulling out. It was observed that number of load cycles until fatigue failure occurred increased with decreasing maximum load for constant minimum load. In addition, the slip at the free bar end is considerably increased during the load cycling, which is mainly influenced by the upper load and the bond length. The authors concluded that the fatigue strength of the bond corresponds to the fatigue strength of centrally loaded concrete. This means that no fatigue bond failure will occur during several million-load reversals if for the usual anchorage lengths required for reinforcements the upper load is smaller than about 50 percent of the static pull-out load. The authors also concluded that the fatigue load affects the bond behavior during service load even if no fatigue failure occurs [28].

Tibetu [29] was carried out a finite element analysis on the effects of both anchorage length and concrete strength on the bond behavior of concrete-rebar connection of bases under low cyclic loading. The model of specimens was prepared to fail by pulled-out by applying fatigue tensile load on reinforcement. The parameters of the study were different concrete strength and anchorage length. The test result showed that applying 78 percent of static load capacity under fatigue conditions resulted in bond failure at the concrete-rebar interface. The result also showed that low cycle fatigue loadings decrease the bond strength of monotonic loading. It was observed that the deterioration of the bond is high when the number of cycles is more than 1000 cycles. Finally, the author concluded that the bond failure governs the failure mode of connection under fatigue loading even if there is an adequate development length provided to resist static loadings [29].

In general, corrosion of reinforcement and cyclic load deteriorates the bond strength because corrosion exerts volumetric expansion on concrete while cyclic load accumulates damages between concrete-rebar interfaces.

### ***2.3.2.3 Improper detailing for bond***

Improper detailing for the bond is another factor that affects the bond of reinforced concrete. The surface condition of reinforcement, the contact area between interface, strength of concrete, diameter of the reinforcement, concrete cover, and transverse

reinforcement are some of the major factors that deteriorate the bond strength due to improper detailing for bond as reported by ACI committee 408 [3]. In this section, these are discussed in detail as follows:

- Concrete cover and reinforcement spacing

The thickness of concrete cover and reinforcement spacing determine the bond strength. Increasing the concrete cover and reinforcement spacing resulted in increased bond strength. In thinner concrete cover and tight reinforcement spacing, the type of failure is splitting failure mode. But, in thicker concrete cover and wider reinforcement spacing, the type of failure is pullout failure. In general, splitting and/or pullout failure modes occur if the provided concrete cover and/or reinforcement spacing are insufficient which then affects bond strength between concrete-rebar interfaces.

- Development and splice length

Decreasing the development and splice length of reinforcement decreases bond strength between concrete-rebar interfaces. Since the bond force is not uniform throughout the member, thus bond failure first occurs in the region where the bond force is high. In anchored reinforcement, bond failure initiates at the extreme surface of concrete or at transverse bending moment cracks where the reinforcement is highly stressed. In the case of spliced reinforcement, splitting failure begins at the end of the splice, which then moves towards the center of the splice. If development and splice length are inadequate, in normal strength concrete, splitting failure occurrence accompanied by crushing of the concrete keys when reinforcement slips concerning concrete, but in the case of high strength concrete and coated reinforcement, the extent of concrete keys crushing is significantly reduced.

- Diameter of reinforcement

A bond strength that developed between concrete-rebar interfaces before bond failure is not only a function of development length, spacing between adjacent reinforcements, and concrete cover, but it is also a function of the cross-sectional area of the reinforcement. The increment of the bond stress at failure is slower than the increment of the area of the reinforcement, thus a longer anchorage length is required for a larger reinforcement size to develop a required bond resistance for given reinforcement stress. Thus, increased development length or splice length is required if the reinforcement diameter increases. In

other words, for a given development length or splice length, a larger reinforcement size achieves a required bond force than smaller size reinforcement for the same amount of confinement. Thus, this shows that area of reinforcement influence the bond strength. The mathematical relationship between reinforcement size and development length is shown in equation 2.8.

$$l_{b,rqd} = \frac{\Phi}{4} * \frac{\sigma_{sd}}{f_{bd}} \quad (2.8)$$

Where  $\Phi$  is bar diameter,

$f_{bd}$  is design bond strength,

$l_{b,rqd}$  is basic development length and

$\sigma_{sd}$  is design stress of the reinforcement at the position from where the development is measured from.

- Reinforcement geometry and surface condition

In history, there is no common view on the effect of reinforcement geometry on bond behavior. Some of the studies reported that deformation on reinforcement surfaces has a strong effect on bond strength. Other studies reported that deformation on the reinforcement surface has little effect. Over time, nevertheless, the effect of reinforcement geometry on bond behavior is increasingly clear. Current studies show that reinforcements with deformed surfaces resulted in higher bond strength than reinforcements with smooth surfaces. Even if studies showed that the load-slip relationship of deformed and smooth reinforcements was the same up to the maximum slip of smooth reinforcements that correspond to the peak bond strength of smooth reinforcements. But, ribs on deformed reinforcement increase the bond strength as slip continued due to the bearing of ribs against concrete keys. In addition, the surface condition of the reinforcement has an important role in bond strength because of the friction effect that exists between the reinforcement and concrete, which transfers bond force. This shows that reinforcement geometry and surface conditions affect the bond strength between concrete-rebar interfaces.

- Concrete properties

Concrete properties also affect bond strength. Tensile strength is one of the concrete properties, which will affect the bond strength. Because bond strength depends on the tensile strength of concrete. Nevertheless, the tensile strength of concrete depends on the compressive strength of concrete; this shows that bond strength is a function of the

compressive strength of concrete. Aggregate type and quality of aggregate are other properties of concrete that influence the bond strength. High strength aggregate and a better quality aggregate in concrete increase the compressive strength of concrete, thus it results in higher bond strength, but lightweight aggregate in concrete decreases the compressive strength of concrete, thus it results in lower bond strength. In addition, an increased slump and admixtures that enhance the workability of concrete reduce the bond strength. In general, concrete properties such as compressive and tensile strength of concrete, type of aggregate used, and the slump of concrete affect bond strength if they are not properly provided.

### **2.3.3 Summary of the Factors that Affect Bond**

In general, environmental conditions and improper detailing of materials influence the bond behavior between concrete-rebar interfaces. Environmental conditions are corrosion of reinforcement and cyclic loading. Corrosions of reinforcement influences bond strength because corroded reinforcement, which is larger in volume, exerts pressure in concrete that results in splitting failure. Accumulation of damage due to several load cycles also reduces the bond strength. During the design period of reinforced concrete structures, improper details or inadequate provision of development length, splice length, concrete cover, spacing between adjacent reinforcements, the diameter of reinforcement, and tensile strength of concrete greatly affect the bond strength.

In addition, missing the concrete spacers and vibration of casted concrete during construction may lead to loss of bond.

## **2.4 Effects of Loss of Bond in Reinforced Concrete**

Mousa [9] carried out an experimental investigation on the effect of loss of bond at main longitudinal reinforcement on the flexural behavior of reinforced concrete beams with different degrees of bond loss in the longitudinal tension reinforcement. To remove a bond action, the longitudinal reinforcements were inserted into the plastic tube before assembling the reinforcements' cage leaving the length behind supports as bonded and at the area where the stirrups cross the main reinforcements. Then, the end of the plastic tube is sealed to prevent the ingress of concrete. Total six simply supported beams were designed to fail in flexure: one beam without shear reinforcement and five beams with shear reinforcement. Two beams from total specimens, one without shear reinforcement

and another with shear reinforcement, were used as reference beams. Beam without shear reinforcement, which was used as the reference beam, was fabricated with the full bond to investigate the failure mode when it was compared with another reference beam with shear reinforcement. In three beams that out of four remaining beams, the unbonded length variation extended from two unbonded spacing between stirrups to six unbonded spacing between stirrups. In the last beam, and six stirrups spacing were unbonded, but it was hooked at the end to develop sufficient anchorage or to prevent excessive slip. Finally, the beams have been tested under static loading. It was observed that there is a significant reduction of cracking load but a moderate reduction of carrying capacity with increasing the loss of bond. It was also observed that the number of cracks reduced but the width of crack increased with the increasing length of unbonded along with the longitudinal reinforcement. Moreover, an increase of mid-span deflection but a decrease of strain is observed as unbonding length increases. The author concluded that the remained bond length in the area where stirrups cross the main longitudinal reinforcement compensates local bond loss between stirrups by creating sufficient bond forces, thus that is the main reason for a moderate reduction in carrying capacity even a significant loss of bonded area [9].

Jeppsson and Thelandersson [30] conducted an experimental investigation on the shear behavior of reinforced concrete beams with loss of bond at main longitudinal reinforcement. To remove a bond effect, the main longitudinal reinforcing bars were inserted into a plastic pipe before assembling of reinforcements' cage leaving the length behind supports as bonded and at the area where the stirrups cross the main reinforcement. Then, the end of the plastic tube is sealed to prevent the ingress of concrete. Total six simply supported beams were designed to fail in shear: one beam without shear reinforcement and five beams with shear reinforcement. Two beams from total specimens, one without shear reinforcement and another with shear reinforcement, were used as reference beams. Beam without shear reinforcement, which was used as the reference beam, was fabricated with the full bond to investigate the difference in the mode of failure between beam with stirrups and beam without stirrups. In the remaining unbonded four beams, the main longitudinal reinforcement was unbonded using a varied plastic tube length, then the reinforcements were hooked at the end to develop sufficient anchorage or to prevent excessive slip. The unbonded length variation extended from one unbonded spacing between stirrups to four unbonded spacing between stirrups. Finally, the beams

have been tested under static loading. It was observed that the reduction of the shear capacity is moderate even if the loss of bond is significant. According to the authors, the reason for the moderate reduction of shear capacity was that the bonded region at stirrups and behind the supports are enough to develop an efficient bond force. In addition, the authors concluded that increasing the number of shear reinforcements is essential in an area where the main longitudinal reinforcement is not bonded because the bond force in the unbonded region redistributes shear reinforcement [30].

Asseged [8] carried out both experimental investigation and finite element analysis on the shear behavior of short reinforced concrete beams with different unbonding lengths of the main longitudinal reinforcement. A plastic pipe was used to remove the bond between the concrete-rebar interfaces. Four deep beams, which were designed to fail in shear, were tested: one beam with fully bonded which was used as a reference beam, and three beams with varied unbonded length (40cm of beam's length unbonded, 80cm of beam's length unbonded and fully unbonded beam). The cross-section of all beams was 20cm width x 30cm height and 180cm overall length, and the span of all beams was 120cm. In all beams, three reinforcements with a diameter of 24mm longitudinal reinforcement at the bottom, two reinforcements with a diameter of 10mm at the top and shear reinforcements with a diameter of 6mm at 200 mm spacing were provided. It was observed that the load-carrying capacity of beams increases with the increase of the unbonded length. It was also observed that the initial cracking load is inversely related to the unbonded length, and the number of cracks decreases as unbonding length increases. Moreover, the failure crack pattern gets flatter, and the beams become more ductile as the length of unbonding increases. Finally, the author concluded that unbonding of the longitudinal tensile reinforcements changes the load transfer mechanism from a combined beam action and arch action to pure arch action [8].

## CHAPTER 3

### EXPERIMENTAL PROGRAM

#### 3.1 General

Reinforced concrete beams were fabricated with loss of bond between reinforcement and surrounding concrete to investigate the shear behavior of slender reinforced concrete beams under monotonic loading. To create the loss of bond between the longitudinal tension reinforcement and concrete, reinforcements were inserted into a plastic pipe to simulate actual bond loss between the reinforcement and surrounding concrete. The shear span to depth ratio ( $a/d$ ) of tested beams was 3.12. The numbers of beams were four, and they were designed to fail in shear. Then, the beams were tested to investigate the effects of the loss of bond on the behavior of reinforced concrete structures, specifically in the shear strength of slender beams.

In this chapter, details of specimens, properties of materials, fabrication methods of specimens and experimental setup are have been presented in detail.

#### 3.2 Details of Specimens

All fabricated beams were 2200 mm overall length with a rectangular cross-section of 200mm width x 300 mm height as shown in figures 3.1 and 3.5. The distance between the supports was 1602mm. Flexural reinforcement consists of three 24 mm-diameter deformed reinforcements at the bottom and two 12 mm-diameter deformed reinforcements at the top. The shear reinforcement having a diameter of 6 mm plain bar with 178 mm spacing was used. The flexural reinforcements were properly anchored at the end to prevent excessive slip between the reinforcement and surrounding concrete. Moreover, additional shear reinforcements are provided to confine longitudinal reinforcements. Concrete spacers were placed underneath and sides of the reinforcement cage at specified positions. The thickness of the concrete cover was 25 mm.

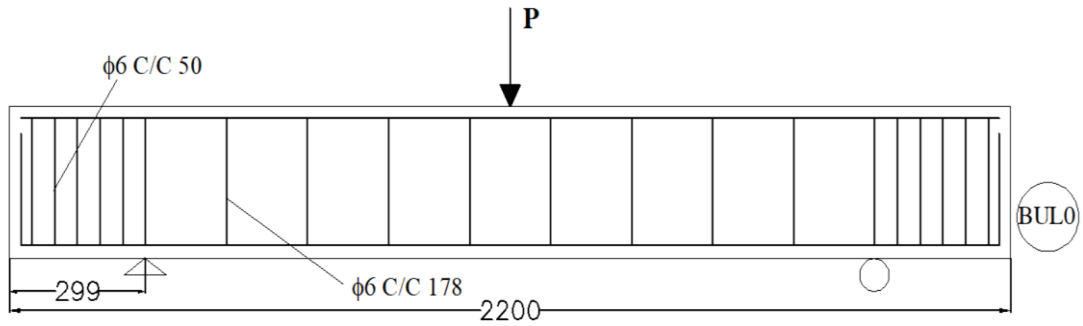


Figure 3-1: Full span bonded beam

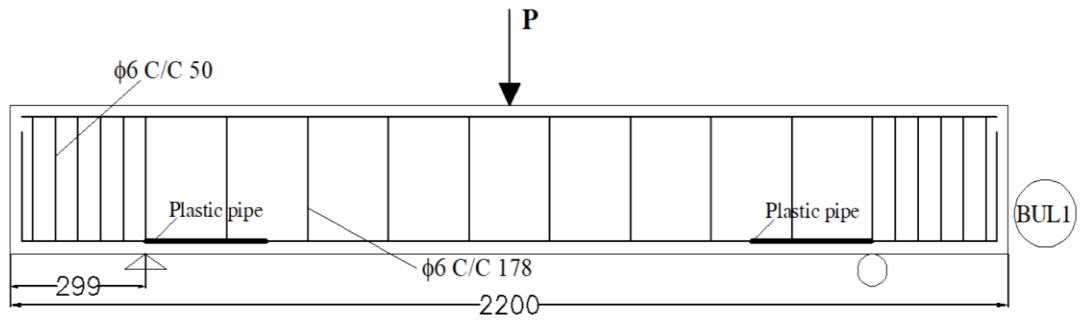


Figure 3-2: One-third of the span unbonded beam

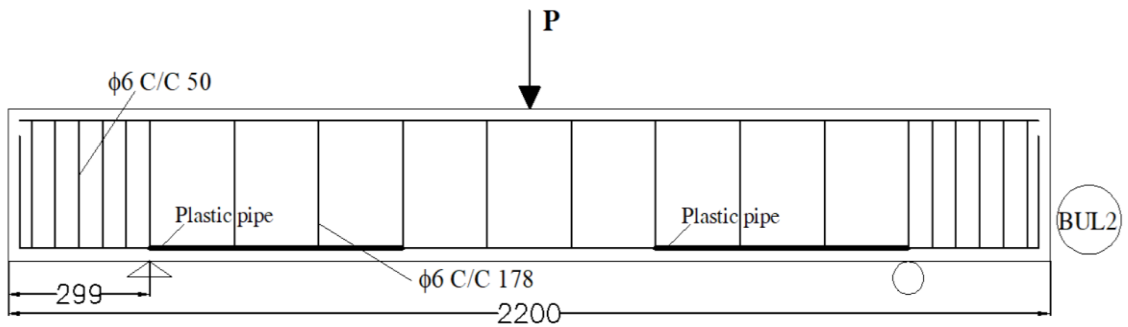


Figure 3-3: Two-third of the span unbonded beam

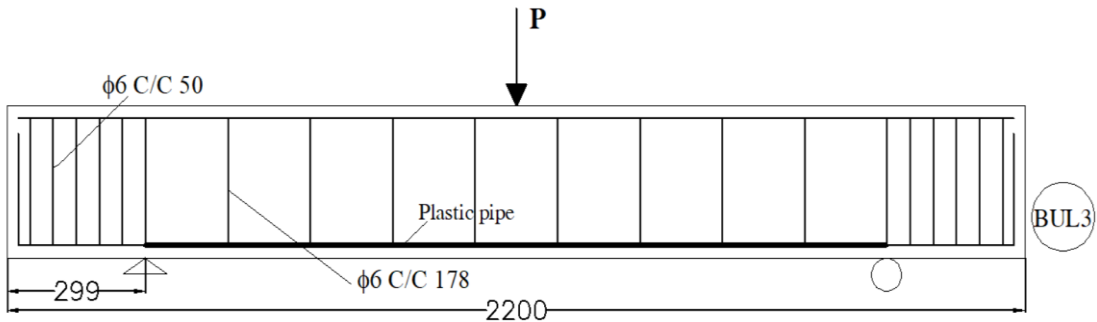
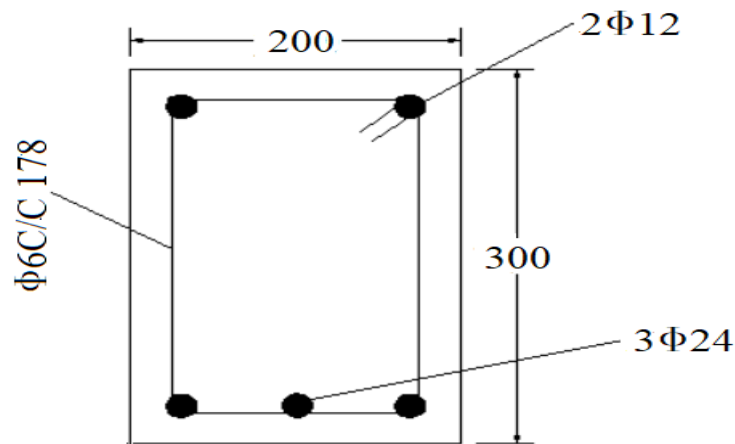


Figure 3-4: Full span unbonded beam



**Figure 3-5: Typical cross-section of a beam**

Three beams out of four were unbonded by inserting reinforcements into the plastic pipe as shown in figures 3.2, 3.3, and 3.4. To identify the beams, designations were given to all beams based on a combination of letters and numbers depending on the acronym of beam's unbonded length and nominator of the ratio of unbonded length to the span of the beam. These designations: full span bonded beam is designated as BUL0, one-third of the span unbonded beam is designated as BUL1, two-third of the span unbonded beam is designated as BUL2, and the full span unbonded beam is designated as BUL3. Where B stands for beam followed by UL that stands for the unbound length of the beam and the number, in the end, is designated by taking the nominator of the ratio of unbonded length to the span of the beam. Control beam (BUL0), which was prepared with the full bonded length of longitudinal reinforcements was used to investigate the failure mode of other unbonded beams.

### 3.3 Property of Materials

#### 3.3.1 Concrete

Concrete was prepared according to the ACI mix design procedure for tested specimens. A mixed proportion of concrete was prepared based on the properties of concreting materials. The quantity of concreting materials used for one cubic meter of concrete is shown in table 3.1. The concrete was specified to have a slump of 50mm, a maximum size of aggregate 25mm, and coarse aggregate was well-graded for good quality of concrete. Ordinary Portland cement was used to prepare specified concrete grades with a water/cement ratio of 0.47. Total twelve concrete cube specimens were cast from the same concrete batch, three for each beam using cube mold size of 150 mm, and another twelve

concrete cylinder specimens were also cast from the same concrete batch three for each beam, using cylindrical mold size of 150 mm diameter and 300mm length. At the time of beam testing, compressive strength was measured by conducting uniaxial compressive tests on the concrete cube specimens shown in figure 3.6, and the concrete tensile strength was also measured by splitting of cylindrical specimens in the same uniaxial compressive tests machine shown in figure 3.7. According to ASTM standard C496 – 96 [31], splitting tensile strength is easy to determine, and its value is greater than the direct tensile strength. The relationship between splitting tensile strength and applied load is shown in equation 3.1. According to ES EN 1992-1-1:2015 [15], direct tensile strength is 90 % of splitting tensile strength. The average compressive strength and 90 % of splitting tensile strength of the concrete are presented in table 4.1, and the complete cube and cylindrical specimens' test results are provided in ANNEX B.

$$\sigma_t = \frac{2P}{\pi ld} \quad (3.1)$$

Where;

$\sigma_t$  = Splitting tensile strength [MPa],

P = Maximum applied load indicated by the testing machine [N],

l = Length of cylindrical specimen [mm], and

d = Diameter of cylindrical specimen [mm].

**Table 3-1: Quantity of materials for mix proportion per cubic meter of concrete**

Materials	Quantity (kg/m <sup>3</sup> )	Percentage (%)
Cement	410.64	16.93
Coarse aggregate	1117.55	46.09
Fine aggregate	702.28	28.98
Water	193.87	8



**Figure 3-6: Compressive strength test**



**Figure 3-7: Splitting test of cylindrical specimen**

**Table 3-2: Summary of the concrete strength**

Beam	Mean cylindrical compressive strength (MPa)	tensile strength(MPa)
Full span bonded beam	45.21	4.75
One-third of the span unbonded beam	44.09	4.56
Two-third of the span unbonded beam	45.67	4.80
Full span unbonded beam	45.67	4.80

### 3.3.2 Reinforcement

The nominal diameters of the reinforcing bars specified in this work were purchased from local suppliers. Then, to determine the mechanical property, the reinforcements specimens were tested in tension in a universal testing machine, and their complete load –elongation was obtained from the test. The tension test was conducted on all the reinforcements used types and three specimens were tested for every reinforcement diameter as shown in figure 3.8. Yield and ultimate tensile strength were computed from test results, and then averaged for each reinforcement diameter as shown in table3.2, and the complete load elongation test results are provided in ANNEX B.



**Figure 3-8: Tensile strength test of reinforcement**

**Table 3-3: Mechanical properties of reinforcements**

Nominal diameter	Average Diameter(mm)	Average yield stress (MPa)	Ultimate tensile stress (MPa)	Elongation, $\epsilon_u$ (%)
6	6.06	397.81	470.61	23.90
12	11.45	666.87	807.08	23.60
24	23.55	626.45	698.71	23.73

### 3.4 Fabrication of Specimens

In this section, all necessary processes to prepare reinforcement cages, formwork, concrete mix and casting of concrete have been dealt with in brief.

#### 3.4.1 Preparation of Reinforcements Cages

The reinforcement cage was prepared for each beam as shown in figures 3.9, 3.10, 3.11 and 3.12. Before anchoring the bottom reinforcements at the end, the first of all reinforcements were inserted into a plastic pipe, which is the used methodology in this study. The spacing of shear reinforcement was closely controlled. Additional shear reinforcements were provided behind supports to prevent excessive slip of longitudinal reinforcement due to loss of bond. All stirrups were anchored with a hook of  $135^\circ$  placed on alternating sides of top longitudinal reinforcements as shown in the following figures. After assembly, the reinforcements' cage was placed in previously prepared wooden formwork.



Figure 3-9: Reinforcement cage of full span bonded beam

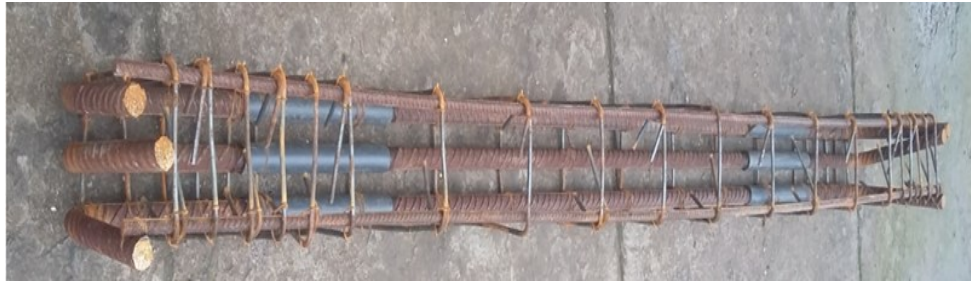


**Figure 3-10: Reinforcement cage of one-third of the span unbonded beam**



**Figure 3-11: Reinforcement cage of two-third of the span unbonded beam**



**Figure 3-12: Reinforcement cage of full span unbonded beam**

### **3.4.2 Preparation of Formwork**

A formwork is prepared from wood materials of straight plywood sheet for soffit and wooden board sheet for side formworks. Both plywood sheet and wooden board sheet were connected at the specified position-using nail as shown figure3.13. The internal dimension of the formwork was fixed with dimensions exactly equal to the specimen dimension and then the formwork had been lubricated with oil for easy removal of the specimen. Before inserting of reinforcements cage in formwork then casting of concrete, the formwork was placed at the level and smooth surface.



**Figure 3-13: Reinforcement cages inside the formwork**

### **3.4.3 Casting of Concrete**

The proportioned concrete ingredients that are shown in table 3.1 were mixed in a concrete mixer until it was uniform in the mixer. Then, the prepared concrete mix was filled into previously prepared formwork and then vibrated to ensure proper consolidation as shown in figure 3.14. As mentioned previously in Section 3.4.1, the reinforcement cage was already placed securely in its proper position in the formwork using 25mm precast concrete cover spacers. The casting of each beam specimen was carried out in two batches. Three cubic and cylindrical specimens were also cast from the same batches to test the compressive and tensile strength of concrete respectively. The formworks were removed after 24 hours of pouring. Then, the beam and the corresponding cube and cylindrical specimens were placed in the same environmental condition and then cured by applying water frequently.



**Figure 3-14: Concrete placing process**

### 3.5 Test Setup

All beams, which were supported with a span of 1602mm, had been tested monotonically applying load at the mid-span of beams. The type of supports was steel plates with the roller on the top of steel plates. A point load was applied at mid-span through hydraulic jack against load cell as shown in figure 3.15, and load points are kept the same for all beams. However, the loading rate was not kept the same because the load was applied manually using a hydraulic jack that was operated using a hand lever. Thus, the loading rate was a little bit varied for every incrementation of load in the same beam. Also, it was not constant from one beam experiment to another beam experiment; however, the effect of loading rate variation was tried to control.

Load cell and LVDT were placed at a specified position to record load and vertical displacement. A loading plate was used to distribute the load uniformly. The load was transferred from the hydraulic jack to the beam through-loading plate as shown in figure 3.15. The surface irregularity of specimens at both supports and loading points was smoothed by using gypsum. Then, the specimen is easily balanced on roller supports and the load cell placed on the horizontal surface of the specimen distributes the load uniformly. In addition, lines were drawn on each beam to show the location of the point loads, supports, and the mid-span of the beam to make it easier to install the beam on the testing machine.

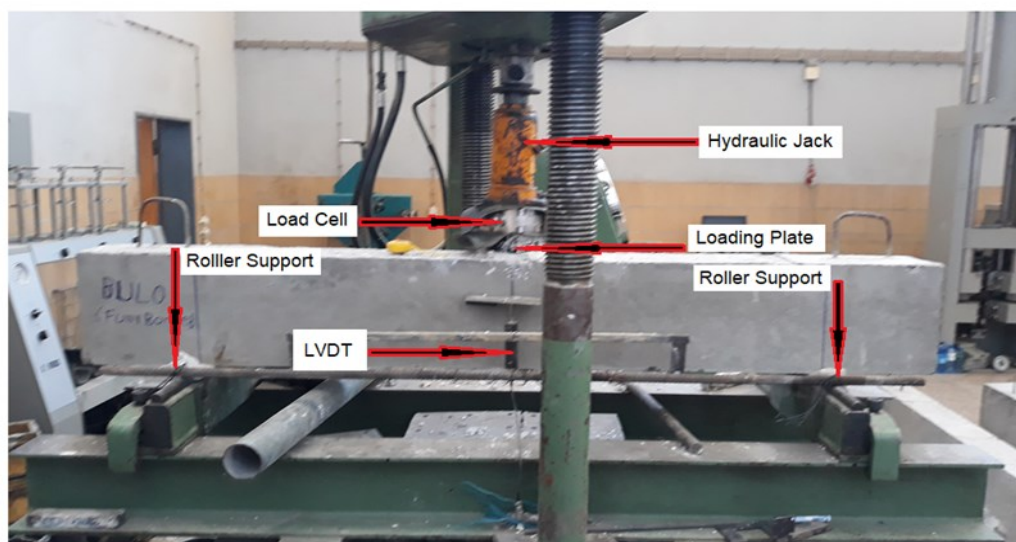


Figure 3-15: Test set up

### **3.6 Instrumentation and Data Acquisition**

Linear variable differential transducers (LVDT's) and load cell were installed to measure mid-span deflection and load, respectively. Hence, before starting testing, linear variable differential transducers (LVDT's) and load cell were mounted at the mid-span of the beam. During the test, the load and the vertical displacement were recorded using a data logger. Finally, the test was stopped once the beam was failed.

## CHAPTER 4

### FINITE ELENRMT ANALYSIS USING VecTor2

#### 4.1 About the Software

For computational simulation and analysis of this study, the VecTor2 finite element analysis platform is used. It is a nonlinear finite element program for the analysis of two-dimensional reinforced concrete membrane structures. Hence, VecTor2 is used to predict the load-deformation response of a variety of reinforced concrete structures exhibiting well-distributed cracking when subject to short-term static monotonic, cyclic, and reverse cyclic loading. The program utilizes an incremental total load, iterative secant stiffness algorithm to produce an efficient and robust nonlinear solution [32].

Originally, VecTor2 employed the constitutive relationships of the modified compression field theory. Subsequent developments have incorporated alternative constitutive models for a variety of second-order effects including compression softening, tension stiffening, tension softening, and tension splitting. In addition, the capabilities of the VecTor2 have been augmented to model bond-slip relationships, reinforcement dowel action, reinforcement buckling, and crack allocation processes.

Finite element models constructed for VecTor2 use a fine mesh of low-powered elements. This methodology has advantages of computational efficiency and numerical stability. It is also well suited to reinforced concrete structures, which require a relatively fine mesh to model reinforcement detailing and local crack patterns. The element library includes a three-node constant strain triangle, a four-node plane stress rectangular element, and a four-node quadrilateral element for modeling concrete with or without smeared reinforcement; a two-node truss-bar for modeling discrete reinforcement; and a two-node link and a four-node contact element for modeling bond-slip mechanisms.

#### 4.2 Material Models

Constitutive models for materials are paramount to the accuracy of the VecTor2 results. At each load step, the structure stiffness is determined from the stresses and strains calculated from the constitutive models of materials. Accordingly, material models have

been incorporated in VecTor2. The models are concrete material models, reinforcement material models, and models for the bond. For each material, different modeling options have been incorporated into the VecTor2 program.

#### 4.2.1 Concrete Models

Different modeling options have been incorporated in VecTor2 for compression pre-peak, compression post-peak, compression softening, tension stiffening, tension softening, and FRC tension. Moreover, modeling options for confinement, lateral expansion, cracking criterion, crack stress calculations, crack width check, crack slip calculation, creep & relaxation and hysteretic response are also available in the program. In this study, the selected modeling options are presented in table 4.1.

**Table 4-1: Summary of the used modeling option for concrete**

Concrete behavior	Used model
Compression post- peak	Hognested (Parabola)
Compression post- peak	Saenz/Sacone
Compression softening	Vecchio-Collins 1982
Tension stiffening	Izumo, Maekawa et al
Tension softening	Bilinear
FRC tension	Not considered
Confinement strength	Kapfer/Richart
Dilation	Variable-Isotropic
Cracking criterion	Mohr-Coulomb (Stress)
Crack stress calculation	Basic(DSFM/MCFT)
Crack width check	Agg/2.5Max Crack Width
Crack slip calculation	waraven
Creep& Relaxation	
Hysteretic response	Nonlinear W/Plastic offsets

#### 4.2.2 Reinforcement Models

VecTor2 has also incorporated different modeling options for reinforcement. Reinforcement models include hysteric response, dowel action, and buckling. In this study, Seckin Model with Bauschinger Effect, Tassios (Crack Slip), and Akkaya 2012 (modified dhakal-Maekawa2002) modeling methods are used to model hysteric response, dowel action, and buckling respectively.

#### 4.2.3 Bond Models

As mentioned in previous chapters, the main objective of this study is to investigate the effect of loss of bond between concrete-rebar interfaces. Bearing this in mind, this finite element aims to examine how the bond will be modeled with the loss of bond using VecTor2 software.

VecTor2 has incorporated the different modeling options to represent the bond stress-slip relationship between concrete-rebar interfaces. In this study, the Eligehausen modeling method is used from the available options.

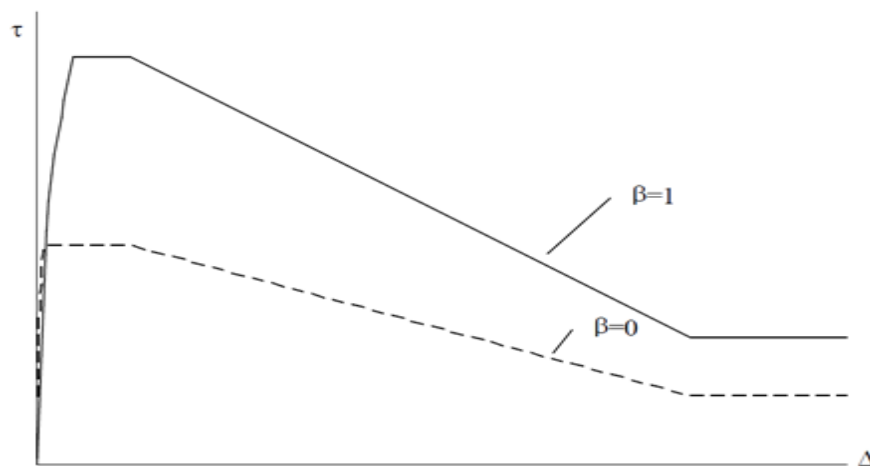


**Figure 4-1; Eligehausen bond stress-slip response**

The model first determines the stress-slip relationship for two distinct cases: confined bars ( $\beta = 1$ ) and unconfined bars ( $\beta = 0$ ). The stronger relationship for confined bars corresponds to pullout type bond failure, whereas the relationship for unconfined bars corresponds to splitting failure. Both the confined and unconfined bond stress-slip relationships are defined by a series of reference bond stresses ( $\tau$ ) and bond slips ( $\Delta$ ). Then, the actual bond stress-slip model is defined by a series of reference bond stresses ( $\tau_{sp}$ ) and slips ( $\Delta_{sp}$ ). These are determined by linearly interpolating between the unconfined and confined

reference bond stresses and slips using the confinement pressure factor ( $\beta$ ). A confinement pressure of zero corresponds to the unconfined case of splitting failure, while a confinement pressure of 7.5 MPa corresponds to the confined case of pullout failure. Based on the anticipated confining pressure ( $\sigma$ ) and the confinement pressure factor may be computed as follows:

$$\beta = \frac{\sigma}{7.5}, \quad (\text{in MPa}) \quad 0 \leq \beta \leq 1$$

### 4.3 Analysis Models

In addition to the modeling of the mechanical properties of materials, structural properties of beams are modeled using the modeling option in table 4.2.

**Table 4-2: Used analysis model**

Analysis behavior	Used method
Strain History	Previous Loading Considered
Strain Rate Effects	C:n/c S:n/c
Structural Damping	Not Considered
Geometric Non linearity	Considered
Crack Spacing	CEB-FIP 1978-Deformed

### 4.4 Material Properties

Mechanical properties of concrete and reinforcement obtained from the experiment were used as input parameters in the finite element program. Because the analytical model was expected to conform to the experimental results. Hence, the concrete strength obtained from the compression and splitting test and tensile strength of reinforcements experimentally obtained from the tension test was directly used as input for the analytical model. For other properties of concrete and reinforcement, VecTor2 default values were used.

## 4.5 Specimens

In this study, the specimen model is created graphically using preprocessor software formworks, which is used to provide a user interface for generating, visualizing, and checking the finite element model. Accordingly, concrete regions are first defined by one or more polygonal regions on formworks platforms. The second step is defining reinforcement paths on the defined regions of concrete. Each reinforcement path is defined by a series of line segments, which are connected to the concrete elements with bond link elements in the region of loss of bond. However, in the bonded region, it is directly connected to concrete elements through nodes.

Four specimens analogous to the experimental beams were modeled. The nomenclature used for experimental beams shall be implemented for the respective specimens. During the experimental study, it was inevitable that there should be some variations in specimen fabrication. However, such discrepancies were not encountered during analytical simulation. Therefore, a more accurate output is expected. Figure 4.2 shows a typical model of finite elements.

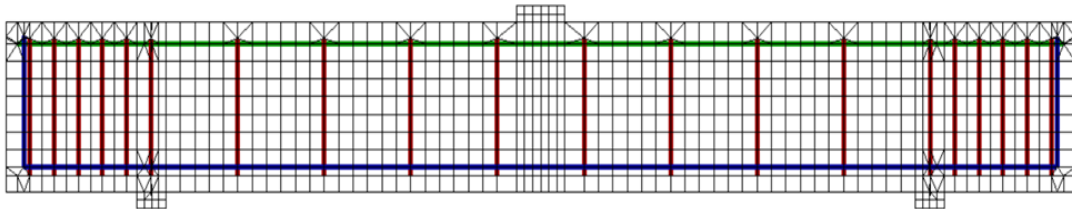


**Figure 4-2: Typical model of finite element**

## 4.6 Analysis of Finite Element Model

The goal of the VecTor2 analysis is to approximate the response of an actual reinforced concrete structure to a given loading scenario and thereby solve a specific engineering question. The approach is to partition the structure into finite elements, generate solutions for each element, assemble the solutions and thereby determine the response of the entire structure.

## CHAPTER 5

### RESULTS AND DISCUSSION

#### 5.1 General

This study focuses on investigating the shear behavior of slender beams, with loss of bond between concrete and longitudinal tension reinforcement, under monotonically increasing load. Four beams, which had been fabricated varying unbonded length, were tested. The beams are full-span bonded beam, one-third of the span unbonded beam, two-third of the span unbonded beam and full-span unbonded beam. In addition, for each beam, the corresponding cubic and cylindrical specimens' compressive and splitting strength were tested respectively. The unbonded region was only created between the supports, but the beam was fully bonded behind the supports to prevent excessive slip due to loss of bond. Moreover, the longitudinal reinforcements had been confined by providing additional stirrups behind supports. All beams have the same cross-sectional area. The support condition was simple support.

As expected, all beams were failed by shear except the fully unbonded beam, which was failed by flexure. Crack patterns, mid-span deflection, and mode of failure were monitored in each beam starting from the initial load to the failure load. In this chapter, test results that were obtained from the data logger were presented and then discussed in detail.

#### 5.2 Experimental Results

##### 5.2.1 Full Span Bonded Beam (BUL0)

A fully bonded beam was used as a reference beam to compare and contrast the shear behavior of other beams, which were fabricated using artificial debonding material to create the loss of bond. It was tested 74 days after fabrication. The beam was monotonically loaded at mid-span under concentrated load, and it was finally failed by shear.

At the early stage of loading, initial flexural-shear cracks appeared around the center of the shear span on both sides of the beam from mid-span. Immediately after these initial flexural-shear cracks, other inclined cracks appeared around neutral depth on both sides of

the beam from mid-span. Then, inclined cracks propagated towards the point of load applied and supports due to further increased loading, and it was started to open widely until the failure. The inclined cracks appeared at a load of 219 kN. As shown in figure 5.1, the fully bonded beam was failed by diagonal tension.



**Figure 5-1: Failure mode of BULO**

Figure 5.2 shows the load versus deflection curve of the fully bonded beam. After the development of inclined cracks, the load versus deflection response curve became flattered due to the reduction of stiffening effect as shown in figure 4.2. The peak load and its corresponding mid-span displacement of this beam are 334.6 kN and 7.85 mm respectively. In addition, after ultimate load, concrete contribution has decreased due to crack, and then the beam was suddenly lost 47% of its load-carrying capacity. However, it carries an additional load by yielding shear reinforcement, and by dowel action of flexural reinforcement before failure.

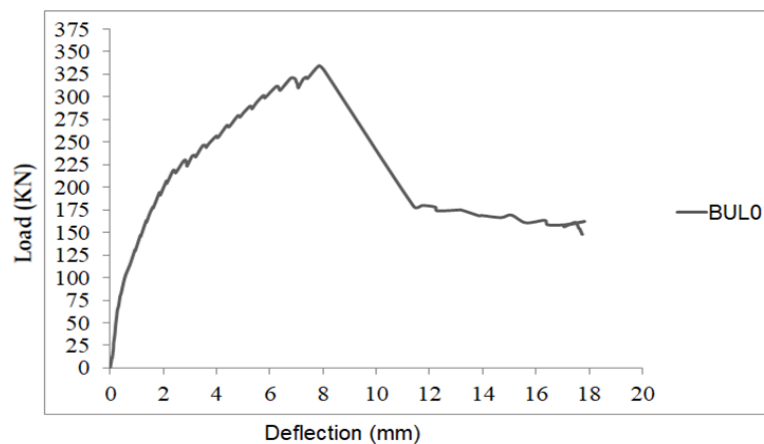


**Figure 5-2: Load versus deflection curve of BULO**

### 5.2.2 One-Third of the Span Unbonded Beam (BUL1)

This beam was tested 75 days after fabrication. It was monotonically loaded at mid-span under concentrated load. Crack patterns, mid-span deflection, and mode of failure were monitored during testing.

At the early stage of loading, small flexural cracks were observed around the mid-span of the beam. As the level of loading increased, flexural-shear cracks were developed at the end of the unbonded length. These flexural-shear cracks appeared at a load of 135 kN. As loading increases further, those flexural-shear cracks propagated to the compression zone with a slight return towards the point of load applied and to the support point by splitting the concrete cover along with the reinforcements, as shown in figure 5.3. At the final stage, shear reinforcement was ruptured; and the beam was suddenly failed by shear. In addition, a concrete cover under the region of unbonded length was spalled out. As shown in figure 5.3, this beam was failed by diagonal tension.

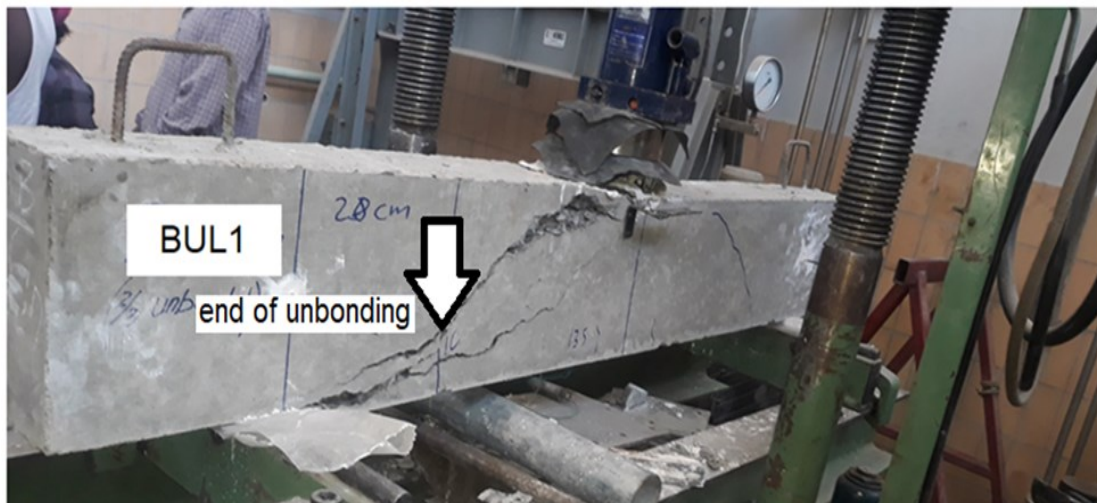


**Figure 5-3: Failure mode of BUL1**

Figure 5.4 shows the load versus deflection curve of the one-third of the span unbonded beam. Until the peak load, the load-deflection response of the one-third of the span unbonded beam exhibited linear behavior. The peak load and its corresponding mid-span displacement of this beam are 197.3 kN and 3.24 mm respectively. The contribution of concrete has decreased after the ultimate load because the tensile strength of concrete approaches zero at the crack. However, this beam continues to carry the additional load by yielding shear reinforcement and dowel action before failure, as shown in figure 5.4.

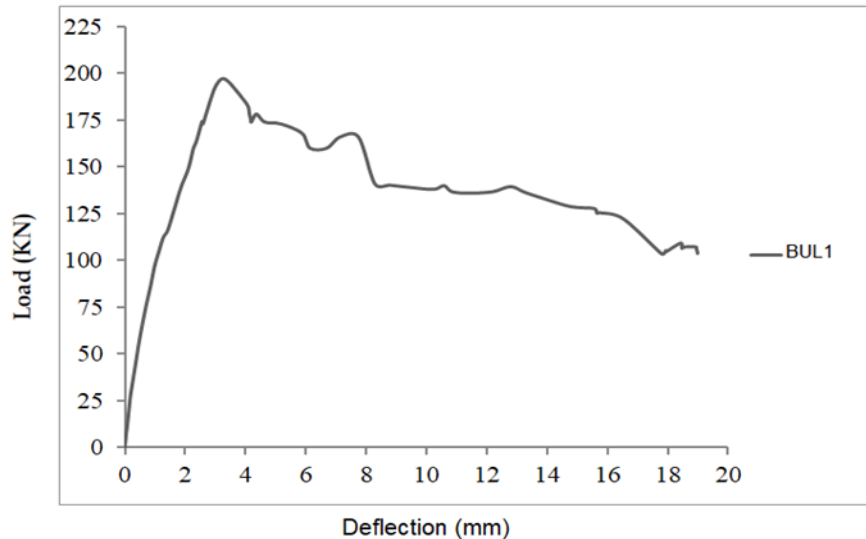


Figure 5-4: Load versus deflection curve of BUL1

### 5.2.3 Two-Third of the Span Unbonded Beam (BUL2)

This beam was tested 78 days after fabrication. It was monotonically loaded at mid-span under concentrated load. Crack patterns, mid-span deflection, and mode of failure were monitored during testing.

At the beginning of loading, initial flexural-shear cracks were developed at the end of the unbonded length. These cracks appeared at a load of 185 kN. As loading increases, those flexural-shear cracks propagated to the compression zone with a slight return towards the point of load applied and to the support by splitting the concrete cover along with the reinforcements, as shown in figure 5.5. At the final stage, cracks opened widely and the beam was suddenly failed by shear. Similar to one-third of the span unbonded beam, the concrete cover under the region of unbonded length is spalled out.

Figure 5.6 shows the load versus deflection curve of two-third of the length-unbonded beam. Like the previous beam (BUL1), the load-deflection response of the two-third of the span unbonded beam exhibited linear behavior starting from initial load to peak load. The peak load and its corresponding mid-span displacement of this beam are 289.4 kN and 6.58 mm respectively. The contribution of concrete has decreased after the ultimate load due to crack. However, this beam carries an additional load by yielding shear reinforcement and dowel action before failure, as shown in figure 5.5.

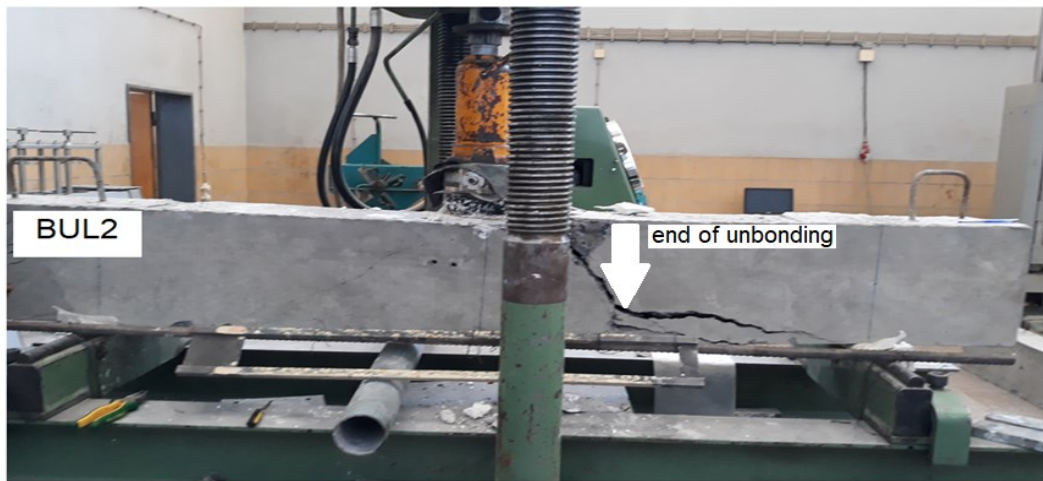


Figure 5-5: Failure mode of BUL2

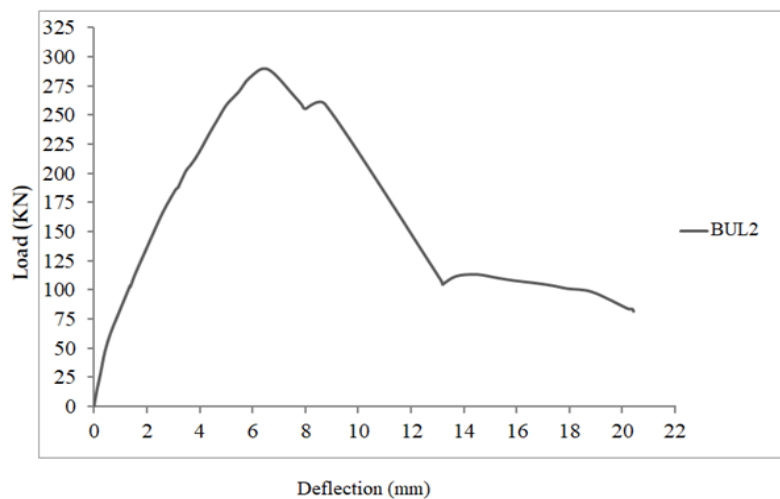


Figure 5-6: Load versus deflection curve of BUL2

#### 5.2.4 Full Span Unbonded Beam (BUL3)

This fully unbonded beam, which was fabricated debonding the full span of the beam, was monotonically loaded at mid-span under concentrated load and its failure mode is shown in figure 5.7. It was tested 76 days after fabrication. Crack patterns, mid-span deflection, and mode of failure were monitored during testing.

Two initial flexural cracks appeared near the mid-span at the beginning of loading. As the level of loading increases, these cracks propagated upwards to the compression zone with a wide opening. The beam was continuously loaded until the load of 423.17 kN. Then, the system of loading was stopped before failure because the used hydraulic jack is not capable to transfer additional load. However, the beam was reloaded again using a higher capacity

hydraulic jack after 8 months to know its mode of failure and ultimate load-carrying capacity. Finally, the beam failed by flexure and its ultimate load-carrying capacity is 441.5 kN in the second cycle test.



**Figure 5-7: Failure mode of BUL3**

Figure 5.8 shows the load versus deflection curve of the full span unbonded beam. The peak load and the corresponding mid-span displacement of this beam are 441.5 kN and 20.89 mm respectively. Moreover, the load-deflection response of the full span unbonded beam exhibited linear before peak load.

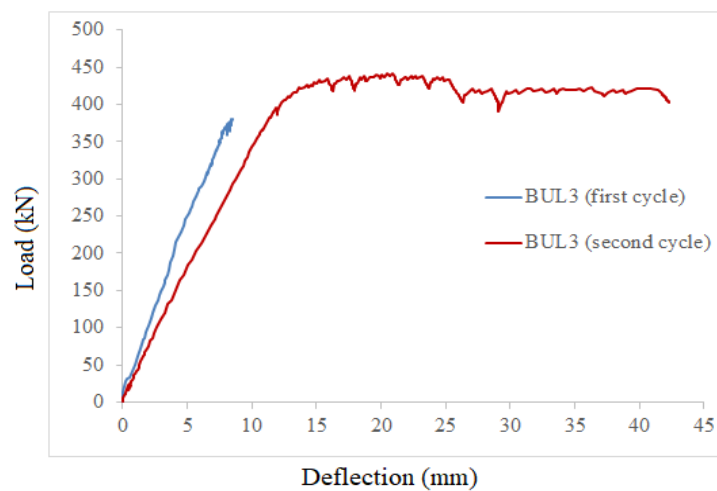


**Figure 5-8: Load versus deflection curve of BUL3**

In the following table, the summary of the experimental results of all beams is presented including the mechanical properties of concrete.

**Table 5-1: Summary of test results**

	Mean cylindrical compressive strength (MPa)	tensile strength(MPa)	Inclined cracking load (kN)	Peak load (kN)	Deflection at peak load (mm)	Failure mode
BUL0	45.21	4.75	219	334.6	7.85	Diagonal-tension
BUL1	44.09	4.56	135	197.3	3.24	Diagonal-tension
BUL2	45.67	4.80	185	289.4	6.58	Diagonal-tension
BUL3	45.67	4.80		441.5	20.89	Flexural

In the case of BUL3, inclined crack is not developed because the mode of failure has been changed from shear to flexure.

### 5.3 Discussion of Results

It was observed that loss of bond between reinforcement and surrounding concrete has significant effects on crack patterns, mode of failure and load-carrying capacity. In the fully unbonded beam (BUL3), two flexural cracks developed and propagated into the compression zone. In the case of partially unbonded beams (BUL1 and BUL2), the formed inclined is steeper than that of the reference beam, and crossed longitudinal reinforcements of the beam at the end of the unbonded length. Also, the load-carrying capacity of the beams has been varied: the load-carrying capacity increased in BUL3 and the load-carrying capacity decreased in BUL1& BUL2. Moreover, failure mode changes from shear to flexure in the case of BUL3. In this section, the effects of loss of bond between reinforcement and surrounding concrete with different percentages of bond loss have been discussed and then compared with the reference beam.

In BUL3, only two flexural cracks were developed in the early-stage loading then opened widely and propagated into the compression zone with increasing levels of load. Besides, crushing of concrete occurred with large deformation of the beam. In this beam, the load-carrying capacity has increased by 31.95%. Beam in this case act somewhat as a tied arch with a thrust line from point load. Thus, the beam transfers the load by arch action, which

enhances the shear load-carrying capacity. That is the reason for the increment of load-carrying capacity. The ultimate load of the beam was 441.5 kN which was 99 percent of its calculated nominal flexural strength load of 446.8 KN.

In BUL1 & BUL2, initial flexural-shear cracks were developed at the end of unbonded length in the early-stage loading. Then as loading increases, those cracks propagated to the top surface of the beam with slight returns towards the load point and horizontally to the support by splitting of concrete cover. The possibility of critical inclined crack to cross shear reinforcements in the shear span is low because the formed inclined crack is steeper than the reference. However, the critical inclined crack crossed all stirrups in the shear span of the control beam. The inclined crack patterns and mode of failure are found to be similar in partially unbonded beams. Besides, it was observed that diagonal failure crack crossed the end of undonded length in shear span. Inclined cracking load increased as partial debonding length increased. Moreover, partial loss of bond has decreased the load-carrying capacity of the beams considered in this work. However, the load-carrying capacity increased as the loss of bond increased. The load-carrying capacity of BUL1 & BUL2 has decreased by 41% and 13.5% respectively when compared with the reference beam. Also, in these beams, shear resistance by web reinforcement is not effective. Because the possibility of inclined crack to cross shear reinforcements in the shear span is low due to the steeper failure inclined crack. This is the cause for the reduction of load-carrying capacity.

Figure 5.9 shows the load versus deflection curve of all beams. It is observed that loss of bond affects the stiffness of beams. In unbonded beams, the stiffness of beams is reduced almost in a linear behavior as loading increases. However, it is reduced at an increasing rate after the development of diagonal cracks in the case of the reference beam. Furthermore, the flexural stiffness of the beams decreases as the percentage of debonding length increases as shown in figure 5.9. This shows that the bond is important to enhance the stiffness of reinforced concrete structures.

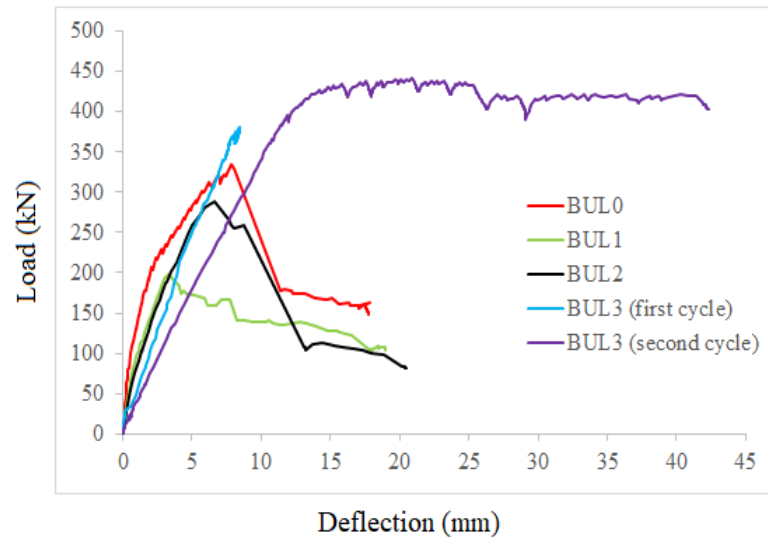


**Figure 5-9: Load versus deflection curve of all beams**

**Table 5-2: Summary of peak loads and their variation from the reference beam**

Beam	Peak Load (KN)	% of variation from fully bonded
BUL0	334.6	
BUL1	197.3	-41
BUL2	289.4	-13.5
BUL3	441.5	31.95

#### 5.4 Finite Element Results

The beams have also been modeled using the nonlinear finite element. Then, the analytical results have been compared with the experimental results. In this section, a combined load versus deflection curves of analytical and experimental results were drawn for comparison and then the relationship between them was discussed in detail.

In the fully bonded beam, both analytical and experimental load versus deflection curves almost approaches each other in pre-peak response, as shown in figure 5.10. However, the post-peak response is varied in the fully bonded beam. In the case of one-third of the span bonded beam, analytical and experimental load versus deflection curves were similar in pre-peak response, as shown in figure 5.11. Moreover, the post-peak response of analytical curve approaches to experimental curve than other beams in one-third span bonded beam.

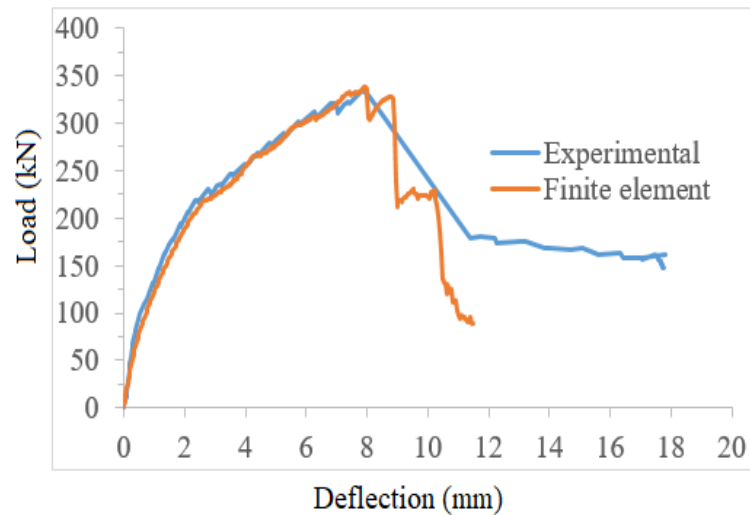


**Figure 5-10: Experimental and analytical load versus deflection curves of BUL0**

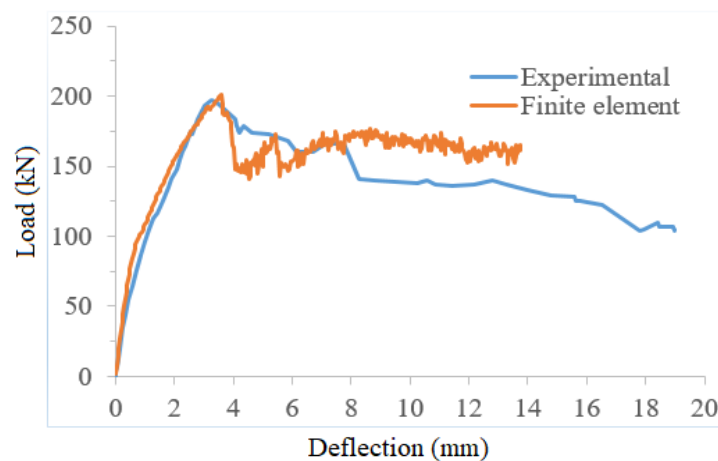


**Figure 5-11: Experimental and analytical load versus deflection curves of BUL1**

Regarding the two-third of the span unbonded beam, load versus deflection responses have coincided in pre-peak response as shown in figure 5.12. In this beam, a little bit lower peak load was observed in the analytical result than in the experimental. Unlike one-third of the span unbonded beam, in two-third of the span unbonded beam, the post-peak response of the analytical curve was significantly varied from the experimental. In the case of a fully undonded beam, analytical and experimental load versus deflection curves were varied both in pre-peak and in post-peak responses, as shown in figure 5.13. Also in this beam, a little bit lower peak load was observed in the analytical result.

In general, a good relationship was observed both in experimental and analytical results especially in pre-peak response. Finite element analysis is found consistent with the experimental result. Hence, it is possible to model beams with loss of bond using bond stress-slip relationships models between the concrete-rebar in finite elements.

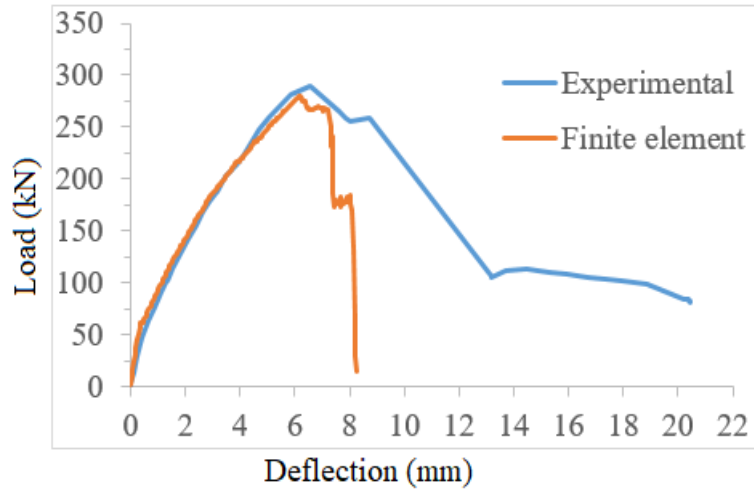


Figure 5-12: Experimental and analytical load versus deflection curves of BUL2

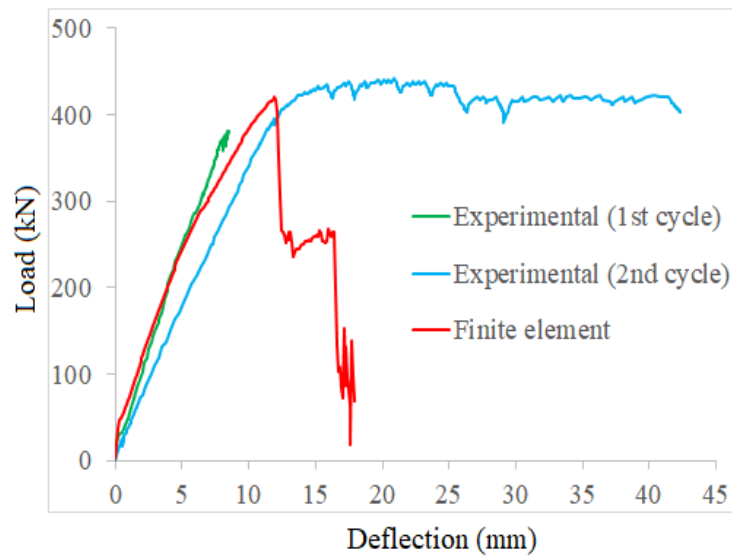


Figure 5-13: Experimental and analytical load versus deflection curves of BUL3

Table 5-3: Peak load comparison of experimental and analytical results

Beam	Experimental Load (kN)	Analytical Load (kN)	% of variation
BUL0	334.6	337.8	0.9
BUL1	197.3	200.5	1.6
BUL2	289.4	279.1	-3.5
BUL3	441.5	419.8	-4.9

## CHAPTER 6

### CONCLUSION AND RECOMMENDATION

#### 6.1 Conclusion

This research work investigates the effects of loss of bond between concrete-rebar interfaces on the shear behavior of slender reinforced concrete beams using experimental investigation and finite element analysis. The obtained from the study have been concluded as follows:

Loss of bond between concrete-rebar interfaces affects the shear load carrying capacity of the reinforced concrete beam. In the case of partially unbonded beams, the load-carrying capacity of the beams decreases; however, the ultimate load-carrying capacity increases as the loss of bond increases. Ultimate load-carrying capacity had decreased by 41% and 13.5% for one-third of the span loss of bond and two-third of the span loss of bond respectively because most web reinforcement is not effective to resist the load as a reference beam due to steeper diagonal failure crack. In the case of the fully unbonded beam, load-carrying capacity has increased by 31.95% because due to the loss of bond the beam acts somewhat as a tied arch with a thrust line from point load, which enhances the shear load-carrying capacity.

Besides, loss of bond varies crack patterns and mode of failure. In the fully unbonded beam, only two flexural cracks develop and propagate to the compression zone. In the case of partially unbonded beams, flexural-shear cracks develop and then propagate to the top surface of the beam with slight returns to point load. The failure diagonal crack of partially unbonded beams is steeper than the reference beam diagonal crack, and these cracks crossed the shear span of the beam at the end of the unbonded length. Moreover, loss of bond changes the failure mode from shear to flexure in the case of the fully unbonded beam.

The flexural stiffness of the beams decreases as the percentage of debonding length increases.

The results of finite element analysis have been consistent with the experimental results.

## 6.2 Recommendation

The effects of loss of bond between concrete-rebar interfaces on shear behavior of slender reinforced concrete beams were studied. Then the following recommendations have been forwarded.

The test result shows that beams with partial unbonded length harm the load-carrying capacity; however, loss of bond enhances load carrying capacity in the case of the fully bonded beam. So that in the case of partial unbonded beams, loss of bond that can create the critical section leads to early failure. Therefore, it must be taken into account during the design and construction of concrete structures since built-up structures were required to sustain at least the design loads during their design period, and it requires further study on the effects of gradually deteriorating bond strength.

Due to the limitation of tested data, it is difficult to generalize the effects of loss of bond on all types of reinforced concrete structures. Therefore, further study is needed by conducting additional tests on different slenderness ratios, material property, and beams with or without web reinforcements.

The current bond strength verification methods assume constant bond strength throughout the design period. Thus, it needs revising to take into account inevitable bond loss during service time in the future.

REFERENCES

- [1] R. F. Warner, B. V. Wangan, A. S. Hall and K. A. Faulkes, *Concretes Structures*, Melbourne, Australia: Addison Wesley Longman, 1998.
- [2] L. N. Lowes, "Finite Element Modeling of Reinforced Concrete Beam-Column Bridge Connections," University of California, Berkeley, 1999.
- [3] ACI Committee 408, "Bond and Development of Straight Reinforcing Bars in Tension," American Concrete Institute, 2003.
- [4] Y. Sun, Z.-x. Gu, A. Li and G.-j. Shao, "Effect of Structural Features and Loading Parameters on Bond in Reinforced Concrete under Repeated Load," *Structural Concrete.*, 2017.
- [5] A. S. Mohammed, "Effect of Cyclic Loadings on the Shear Strength and Reinforcement Slip of RC Beams," *Civil Engineering Journal*, vol. 3, no. 2, 2017.
- [6] E. Gebreyouhannes, T. Yuya and K. Maekawa, "A Poro Mechanical Approach for Assessing the Structural Impacts of Corrosion in Reinforced Concrete Members," in *Proceedings of the 1st International Conference on Ageing of Materials & Structures*, Delft, The Netherlands, 2014.
- [7] S. Li, F. Zhiwei and H. Jian, "Experimental and Analytical Investigation of the Fatigue Flexural Behavior of Corroded Reinforced Concrete Beams," *International Journal of Concrete Structures and Materials*, 2019.
- [8] T. Asseged, "Effect of Loss of Bond on the Shear Behavior of Short Reinforced Concrete Beam," Addis Ababa University Institute of Technology, Addis Ababa, Ethiopia, 2012.
- [9] M. I. Mousa, "Effect of bond loss of tension reinforcement on the flexural behaviour of reinforced concrete beams," *Housing and Building National Research Center Journal*, vol. 12, p. 235–241, 2016.

- [10] J. K. Wight and J. G. Macgregor, Reinforced Concrete Mechanics and Design, 5 ed., New Jersey: Pearson Education, 2009.
- [11] M. P. Collins, D. Mitchell, P. Adebar and F. J. Vecchio, "A General Shear Design Method," *ACI Structural Journal*, vol. 93, no. 1, pp. 637-668, 1996.
- [12] M. P. Collins, E. C. Bentz, P. T. Quach, A. W. Fisher and G. T. Proestos, "Predicting the Shear Strength of Concrete Structures," in *The New Zealand Concrete Industry*, Rotorua, 2015.
- [13] ACI Committee 318, "Building Code Requirements for Structural Concrete (ACI 318-02) and Commentary on Building Code Requirements for Structural Concrete (ACI 318R-02)," 2002.
- [14] CSA-A23.3-04, "Canadian Standards Association, CSA-A23.3-04: Design of Concrete Structures," Canadian Standards Association, 2004.
- [15] ES EN 1992-1-1, "Ethiopian Building Code Standard, ES EN 2: Design of Concrete Structures," Ministry of Urban Development & Construction., Addis Ababa, Ethiopia, 2015.
- [16] M. Sinik and G. Arslan, "Effect of Shear Span-to-Effective Depth Ratio on the Shear Strength of RC Beams," in *Proceedings of 142nd IASTEM International Conference*, Antalya, Turkey, 2018.
- [17] A. H. Nilson, D. Darwin and C. W. Dolan, Design of Concrete Structures, 14 ed., New York: Mc Graw Hill, 2010.
- [18] P. M. Ferguson, J. E. Breen and J. O. Jirsa, Reinforced Concrete Fundamentals, 5 ed., New York: Ohn Wiley and Sons, 1988.
- [19] R. Park and T. Paulay, Reinforced Concrete Structures, New York: John Wiley & Sons, 1975.

- [20] X. Wang and X. Liu, "Bond Strength Modeling for Corroded Reinforcement in Reinforced Concrete," *Structural Engineering & Mechanics*, vol. 17, no. 6, pp. 863-878, 2004.
- [21] A. A. Almusallan, A. S. Al-Gahtani, A. R. Aziz and Rasheeduzzafar, "Effect of Reinforcement Corrosion on Bond Strength," *Construction and Building Materials*, vol. 10, no. 2, pp. 123-129, 1996.
- [22] Y. Berthaud, A. Ouglova, F. Foc, M. Francois, F. Ragueneau and I. Petre-Lazar, "Influence of Corrosion on Bond Properties between Concrete and Reinforcement in Concrete Structures," *Materials and Structures*, pp. 969-980, 2008.
- [23] Federation International du Beton (fib), "Bond of Reinforcement in Concrete, State-of-Art Report," International Federation for Structural Concrete, Switzerland, 2000.
- [24] L. Amleh, "Influence of Corrosion of Reinforcing Bars on the Bond between Steel and Concrete," McGill University, Montreal, Canada, 1996.
- [25] M. Tahershamsi, "Structural effects of Reinforcement Corrosion in Concrete Structures," Chalmers University of Technology, Gothenburg, Sweden, 2016.
- [26] A. K. Azad, A. Shamsad and S. A. Azher, "Residual Strength of Corrosion – Damaged Reinforced Concrete Beams," *ACI Materials Journal*., vol. 104, no. 1, pp. 40-47, 2007.
- [27] Z. Ye, W. Zhang, Y. Hu and X. Gu, "Experimental Study on Effects of Fatigue Loading History on Bond Behavior between Steel Bars and Concrete," *Key Engineering Materials*, vol. 711, pp. 673-680, 2016.
- [28] G. Rehm and R. Eligehausen, "Bond of Ribbed Bars under High Cycle Repeated Loads," *ACI Journal*, pp. 297-309, 1979.
- [29] T. Tibebu, "Bond Behaviour of Steel-Concrete Connection of Bases under Fatigue Loading," Addis Ababa University Institute of Technology, Addis Ababa, Ethiopia, 2018.

- [30] J. Jeppsson and S. Thelandersson, "Behavior of Reinforced Concrete Beams with Loss of Bond at Longitudinal Reinforcement," *ASCE Journal of Structural Engineering*, vol. 129, no. 10, pp. 1376-1383, 2003.
- [31] ASTM Standards C 496 – 96, "Standard Test Method for Splitting Tensile Strength of Cylindrical Concrete Specimens," 1996.
- [32] P. S. Wong, F. J. Vecchio and H. Trommels, *Vector2 & Formworks User's Manual*, 2 ed., August 2013.

### APPENDIX A: Concreting materials tests

Physical tests on the concreting materials were conducted. Concreting materials are tested according to ASTM standards and the results are presented below in the tabular form.

#### I. Silt content of sand:

- Silt content of sand

Silt content			
	Frist sample	Second sample	Third sample
Volume of silt (ml)	10	10	15
Volume of sand (ml)	325	320	335
Percent of silt	3.07	3.13	4.48
The average percent of silt	3.56		

#### II. Sieve analysis:

- For coarse aggregate

Sieve size (mm)	Weight of sieve (gm)	Weight of sieve and retained (gm)	Weight of retained (gm)	Percent retained (%)	Cumulative Coarser (%)	Cumulative Passing (%)
37.5	1079	1079	0	0	0	100
25	1170	1360.80	190.80	9.553	9.553	90.447
19	1387	2103.25	716.25	35.861	45.418	54.582
12.5	1161	2092.10	931.10	46.618	92.036	7.964
9.5	1163	1284.14	121.14	6.065	98.101	1.899
4.75	1159	1195.01	36.01	1.803	100	0
Pan	736	736	0	0	100	0
Total			1997.3			

- For fine aggregate

Sieve size	Weight of sieve (gm)	Weight of sieve and retained (gm)	Weight of retained (gm)	Percent retained (gm)	Cumulative Coarser (%)	Cumulative Passing (%)
9.50mm			0	0	0	100
4.75mm	426.30	0	0.60	0.120	0.120	99.880
2.36mm	387.50	426.90	21.20	4.232	4.352	95.648
1.18mm	525.50	408.70	95.0	18.966	23.318	76.682
600 $\mu$ m	324.50	620.50	215.60	43.043	66.361	33.639
300 $\mu$ m	303.50	540.10	135.50	27.051	93.412	6.588
150 $\mu$ m	274.60	439.00	24.10	4.811	98.223	1.777
Pan	416.70	298.80	8.90	1.777	100	0
Fineness modulus = 2.857856						

III. Dry unit weight of Course aggregates:

Dry rodded density = 1673.835 kg/m<sup>3</sup>

IV. Moisture content:

- For coarse aggregate

Moisture content of coarse aggregate	gram (gm)
Weight of wet coarse aggregate	2000
Weight of dry Coarse aggregate	1989.7
Moisture content (%)	0.518

- For fine aggregate

Moisture content of fine aggregate	gram (gm)
Weight wet fine aggregate	500
Weight of dry fine aggregate	472.8
Moisture content (%)	5.75

V. Specific gravity and absorption:

- For coarse aggregate

Mass (mm)		Specific gravity and absorption	
oven-dry (A)	5080.24	Bulk specific gravity (OD)	2.648
SSD (B)	5117.29	Bulk specific gravity (SSD)	2.667
water immersed (C)	3198.64	Apparent specific gravity	2.700
		Absorption Capacity	0.729

- For fine aggregate

Mass (mm)		Specific gravity and absorption	
oven-dry (A)	473.83	Bulk specific gravity (OD)	2.279
SSD (B)	734.09	Bulk specific gravity (SSD)	2.405
water immersed (C)	1026.21	Apparent specific gravity	2.607
		Absorption Capacity	5.520

### APPENDIX B: Mechanical property of materials

Mechanical properties of concrete cube and cylinder samples and reinforcing bars were tested.

#### 1) Concrete Strength

##### i. Specimens of BUL0

- Compressive strength

Specimen	Mass (kg)	Density (kg/m <sup>3</sup> )	$f_{cm}$ (MPa)
1	8.275	2451.85	43.98
2	8.578	2541.63	45.22
3	8.402	2489.48	46.41
mean			45.21

- Tensile strength

Specimen	Mass (kg)	Load (kN)	$f_{tcm}$ (MPa)
1	13.148	244.3	5.17
2	13.123	201.5	3.92
3	13.086	251.2	5.17
mean			4.75

##### ii. Specimens of BUL1

- Compressive strength

Specimen	Mass (kg)	Density (kg/m <sup>3</sup> )	$f_{cm}$ (MPa)
1	8.374	2481.19	43.03
2	8.382	2483.56	43.80
3	8.312	2462.81	45.44
mean			44.09

- Tensile strength

Specimen	Mass (kg)	Load (kN)	$f_{icm}$ (MPa)
1	13.386	244.40	4.88
2	12.959	219.70	4.33
3	13.363	225.32	4.48
mean			4.56

iii. Specimens of BUL2

- Compressive strength

Specimen	Mass (kg)	Density (kg/m <sup>3</sup> )	$f_{cm}$ (MPa)
1	8.477	2511.90	46.16
2	8.549	2533.04	46.92
3	8.556	2535.11	43.94
mean			45.67

- Tensile strength

Specimen	Mass (kg)	Load (kN)	$f_{icm}$ (MPa)
1	13.016	260.59	5.20
2	13.144	211.90	4.23
3	13.895	248.53	4.96
mean			4.80

iv. Specimens of BUL3

- Compressive strength

Specimen	Mass (kg)	Density (kg/m <sup>3</sup> )	$f_{cm}$ (MPa)
1	8.477	2511.90	46.16
2	8.549	2533.04	46.92
3	8.556	2535.11	43.94
mean			45.67

- Tensile strength

Specimen	Mass (kg)	Load (kN)	$f_{cm}$ (MPa)
1	13.016	260.59	5.20
2	13.144	211.90	4.23
3	13.895	248.53	4.96
mean			4.80

2) Tensile strength of reinforcing bars

D(mm)	D2(mm)	Yield load(kN)	Failure load(kN)	Yield stress(MPa)	Failure stress(MPa)	Elongation (%)
6.05		11.40	12.9	396.56	448.73	23.90
6.03		10.60	12.70	371.18	444.71	23.80
6.09		12.40	15.10	425.69	518.39	24.00
				397.81	470.61	23.90
11.47	12.69	69.70	82.40	674.55	797.46	23.70
11.42	12.74	68.40	83.90	667.78	819.11	23.60
11.46	12.79	67.90	83.00	658.28	804.67	23.50
				666.87	807.80	23.60
23.52	25.10	269.70	298.40	621.75	686.81	23.60
23.55	25.40	272.40	308.50	625.37	708.24	23.90
23.57	25.20	276.30	305.90	633.25	701.80	23.70
				626.45	698.71	23.73